RESCUE Rollers: A Platform for Collaborative, Multi-robot Exploration in Search and Rescue

Sidney Nimako-Boateng

CMU-RI-TR-25-21

April 16, 2025

The Robotics Institute
School of Computer Science
Carnegie Mellon University
Pittsburgh, PA

Thesis Committee:

Zeynep Temel, *Co-chair*
Melisa Orta Martinez, *Co-chair*
Aaron Johnson
Ananya Rao

Submitted in partial fulfillment of the requirements for the degree of Master of Science in Robotics.

To my mother for all her support, to Jason and Justin for letting me follow them all those years, to Sebastian for keeping me sane and inspiring me with all your passion. To all my undergrad friends who encouraged me and helped me grow into this program. To Eric, Abby, Anna and Suzanne.

To the few who've been with me since the start of my CMU journey: Michaela, Chris, Jennifer and Janice.

To Rodney Copperbottom, Baymax, and 13 year old Sidney. Nea onnim no sua a ohu.

Abstract

The use of robotic platforms for search and rescue remains a significant challenge for many roboticists. While human and animal first responders play critical roles, their effectiveness can be limited by biological constraints. Robotic systems offer the potential to overcome these limitations, especially in environments that are inaccessible to humans and animals due to size or safety concerns. However, individual robots often struggle to meet the diverse demands encountered during deployment. One promising approach is to deploy teams of robots, each specialized to handle different aspects of the task. In this work, we investigate heterogeneous teams in which members collaborate to accomplish tasks that no single system could achieve alone. We present the design of the Rapid Emergency Search in Cluttered and Unstructured Environments (RESCUE) rollers—a low-cost robotic platform developed to explore collaborative teaming. Our system combines inflatable vine robots and RESCUE rollers to enable locomotion across varied terrain. Additionally, we introduce design enhancements that allow multiple RESCUE rollers to coordinate and perform more complex mobility tasks. By improving mobility, enabling sensing and intelligence, and maintaining scalability through low-cost design, this work aims to enhance the effectiveness of robotic teams in search and rescue operations.

Acknowledgments

This work would not be possible without Zeynep Temel, Melisa Orta Martinez, and Shashwat Singh. I would also like to express special thanks to Laura Blumenschien, Sicheng Wang, Mustafa Ugur, Olivia Sobek, Max Kramer, Isaac Osei, Guadalupe Bernal, and Kiran Marques.

Thank you to all my friends and colleagues in the SHRED and Zoom labs. The journey wouldn't have been half as fun without the people. A particular thanks to Sarvesh for all his mentorship and guidance throughout my masters.

Funding

This work was supported by the National Science Foundation (NSF Grant #2308653)

Contents

List of Figures

List of Tables

Chapter 1

Introduction

For more than 20 years leveraging robotics for search and rescue has been a longstanding objective. As cities become denser, the danger of natural and man-made disasters increases. Robotic systems can supplement the capabilities of human and animal first responders in search and rescue scenarios. They can be leveraged in cases where other responses cannot be used due to environmental dangers or space constraints. In these situations, robots can serve as autonomous or tele-operated scouts collecting information on the environment to share with responders or manipulate inaccessible environments.

Regardless of the specific task and autonomy levels, a valuable search and rescue robot must be capable of handling the diverse locomotive requirements of its environment. In a single deployment a robot can encounter steep inclines, sharp drops, rough terrain and tight turns. Creating a single system that can tackle all of these objectives poses a challenge.

Rather than rely on a single limited agent, we can use multiple agents that in combination can extend their mutual operational domain [21, 35, 36]. Alternatively, researchers have designed systems that change their morphology to adjust to a specific tasks [18, 19, 22, 27]. These attitudes converge in the concept of modular and reconfigurable robots (MRR).

A different strategy is to use a variety of robots with distinct skills and assign tasks to robots based on their strengths.Using teams of heterogeneous robots [25, 33] we can apply individual robots expertise where needed to make up for another's

Figure 1.1: The top presents KOHGA3 robot deployed during the 2011 Japanese Earthquake on various terrains (Image courtesy of IEEE Spectrum). Below we have Boston Dynamic's Spot robot on a test environment simulating a disaster.

weaknesses. In many cases, this involves partitioning the task and assigning different objectives to different robots.

Fearing et al. [11] approximates a robot collectives capability as the product of mobility, intelligence and quantity. In this work, we develop strategies to improve mobility and quantity while making affordances for future development on intelligence amplification. We focus on locomotive challenges for small robots[28, 30] and evaluate how we can reduce the limitations of robotic teams using collaborative actions. We present the design of the Rapid Emergency Search in Cluttered and Unstructured Environment (RESCUE) rollers, a collection of centimeter-scale micro robots designed to assist first responders in locating survivors and allocating resources. We evaluate the RESCUE rollers as part of a heterogeneous team containing Vine robots[4, 12], and extend on their capabilities using modularity and reconfiguration to improve mobility.

Chapter 2

Background

Search and rescue robots can be broadly categorized along two primary dimensions: morphology and function.

In terms of function, robots are primarily assigned tasks such as reconnaissance and mapping, environment search, structural inspection and direct intervention [23]. In all cases, save for direct intervention, the goal of the robot is to collect and relay information about the environment to first responders. This helps ensure they can safely enter spaces to pursue survivors and focus their resources on promising locations. In the direct intervention case, the robot is used to augment the environment or complete repairs in inhospitable or inaccessible places. This could take the form of removing debris and rubble to create paths for first responders or interfacing with nuclear infrastructure.

During the Fukushima Daichii meltdown robotic systems were used for several of these tasks. One system was used to clear debris to allow access to the site, while others were used to remove nuclear waste, monitor gauges within the reactor site, and complete reconnaissance on the site [23].

Morphology can be classified by size. We can distinguish between small systems, easily carry-able by an individual and termed "man-packable"; larger systems that require one or more operators to carry them "man-portable" and the largest "maxi" systems. Both unmanned aerial vehicles (UAVs) and unmanned ground vehicles (UGVs) exist across this spectrum. As size and weight increase, so do payload capacity, compute, and cost each bringing benefits and drawbacks. While UAVs are

Figure 2.1: Existing systems that have found use in search and rescue. from left top right, top to bottom we have the ANYMal (courtesy of ANYbotics AG), the ARCOS system (courtesy of the Mine Safety and Health Administration), a customized remote control car platform and a snakebot (both courtesy of the CMU Biorobotics lab)

a promising area of research for search and rescue, in this work we concentrate on ground-based systems.

A variety of locomotion approaches have been taken for UGVs. Quadrupeds have shown promise in navigating man-made environments and are agnostic to cm-scale terrain variations [14, 34]. However, these robots are often large ($> 0.5m$ along the characteristic dimension) and expensive ($> \$10,000$). Tracked and wheeled systems have been borrowed from other domains including bomb disposal and have similar tradeoffs [25].

Both size and cost limit the deployment scale and flexibility of these systems. Size in particular creates challenges around deployment and transportation. An additional motivation for small size is given by previous work showing that survivors are frequently located in areas called voids which have tight size constraints to enter [31]. A compact form factor also enables locomotion through pipes or other small areas rather than surmounting large obstacles [15].

However, miniaturization creates constraints on system resources. The small

Figure 2.2: A collection of robot teams used for DARPA's SubT challenge or RoboCup Rescue Leagues. From left to right, The Explorer Darpa SubT team, CTU-CRAS-NORLAB's team and Hector's team from RoboCup Rescue League (Multi-Agent Systems for Search and Rescue Applications, Drew (2021))

packaging minimizes the size of the drivetrain, actuators, compute, and power systems, limiting the capabilities of the system to explore its environment. Designing a single agent that can handle the myriad of sometimes mutually exclusive requirements in search and rescue remains a challenge.

To address these challenges more systems, specifically targeting search and rescue, have been produced and tested in field experiments for SAR. One particularly promising design for USAR applications is vine robots [4, 12]. Vine robots' use an inflatable construction and a pressurized air source to move. This enables them to cover large distances, overcome terrain variations and obstacles, and compress to enter tight spaces. They also offer long runtimes, so long as their air supply remains intact. One weakness arises in maneuverability. There are existing solutions to steer vine robots such as pouch motors or tethers, however, these create large arcs to turn the bine robot which limit their feasibility in tight environments [2, 6]. Including sensing capabilities for vine robots also proves difficult due to the lack of fixtures to mount them and the need to route cabling.

Utilizing teams of distinct robots provides another angle for attacking the USAR problem. Using a collection of robots for search and rescue has been explored as a solution to the diverse performance requirements [8, 9, 20]. Recently as part of the Defense Advanced Research Projects Agency (DARPA) Subterranean (SubT) Challenge a variety of teams competed with systems with various morphologies including legs, tracks, wheels, and aerial systems. Team CERBERUS employed

multiple sizes of aerial multi-rotors to scout ahead and explore areas not accessible by their ground based systems [33]. [25] took a similar approach but exchanged CERBERUS' quadruped robots for a combination of tracked robots and hexapods. In both cases, these robots partitioned the environment either temporally or spatially, completing distinct tasks in parallel or working sequentially on a single task. We do not see collaborative behavior towards a shared task. Furthermore, the high cost of the advanced platforms used limits the accessibility and scalability of such multi-robot teams.

This thesis presents the Rapid Emergency Search in Cluttered and Unstructured Environments (RESCUE) roller, a low-cost, man-packable robot for search and rescue that leverages the ideas of both modularity and reconfigurability. We specifically target the tasks of reconnaissance, mapping, and search in zones where the characteristic dimension of the environment is less than twice the characteristic dimension of the agent [23]. We use this platform to explore heterogeneous teaming with explicit collaboration, enabling teams to accomplish tasks that no individual robot could perform alone.

Chapter 3

RESCUE Roller Ant

We noted that many of the shortcomings of micro-robots discussed in 2, namely tackling large scale environment variation, runtime, and covering large distances, are directly addressed by vine robots. Conversely, fine grained movement, and sensing, two limitations of the vine robot are strengths of the micro-robot system. To leverage the complementary capabilities of both platforms, we enable physical interaction between the two, allowing for collaborative behaviors that exceed the individual capabilities of either system. We propose a novel mode of cooperation in which the vine robot functions as transportation infrastructure for the RESCUE rollers. In turn, the rollers assist the vine by guiding its movement, using pushing and pulling actions to steer it toward target locations. To explore and characterize this symbiotic relationship, we design and implement an initial version of the RESCUE roller, which we refer to as the Ant.

3.0.1 Design Overview

Our key objectives in designing the Ant were to preserve a small footprint, ensure independent mobility, and provide sufficient strength to steer the vine robot. A compact form factor minimizes interference with the vine robot's motion and allows access to confined voids that are inaccessible to many other systems. Independent mobility is essential for the rollers to navigate the environment, collect data, and relay information to responders. While we capitalize on the vine robot for large-

scale traversal, the rollers must be capable of localized exploration on their own. Finally, the rollers' strength is critical to enabling physical collaboration with the vine robot; as such, we carefully balanced drivetrain design parameters to ensure adequate performance. Below we expand on the experiments we conducted to determine an wheel design to balance force application to steer the vine robot, gap crossing, slope performance, and obstacle traversal. We also discuss other design decisions relating to sensing and power.

3.0.2 Mechanical Design

Figure 3.1: Photograph of an assembled RESCUE Roller Ant

Towards our size objective, we design the chassis of the RESCUE rollers to minimize the cross sectional area. The chassis houses two Pololu High Power Carbon Brush (HPCB) 250:1 Gear motors as well as a custom PCB. While tank treads are a common choice for these environments [3], as the treads allow you to remain undisturbed by large obstacles and terrain variations, they are also prone to mechanical

failure. In particular, tread detachment has accounted for several failures in the field [23]. As a result we selected a two wheeled differential drive system. A differential drive system preserves our maneuverability, crucial for steering the vine, without requiring additional actuators. The chassis is manufactured from Fused Deposition Material (FDM) 3D Printed Polylactic Acid (PLA). This ensures we can rapidly and affordable manufacture the RESCUE Rollers, improving their accessibility. To stabilize of the RESCUE Roller when it moves, and to prevent tipping when it climbs obstacles, the robot also includes a tail, extending 84 mm behind the front surface of the robot and housing a 3.7 V 1000 mAh lithium polymer battery. With this configuration we have a theoretical runtime of approximately 2 hours.

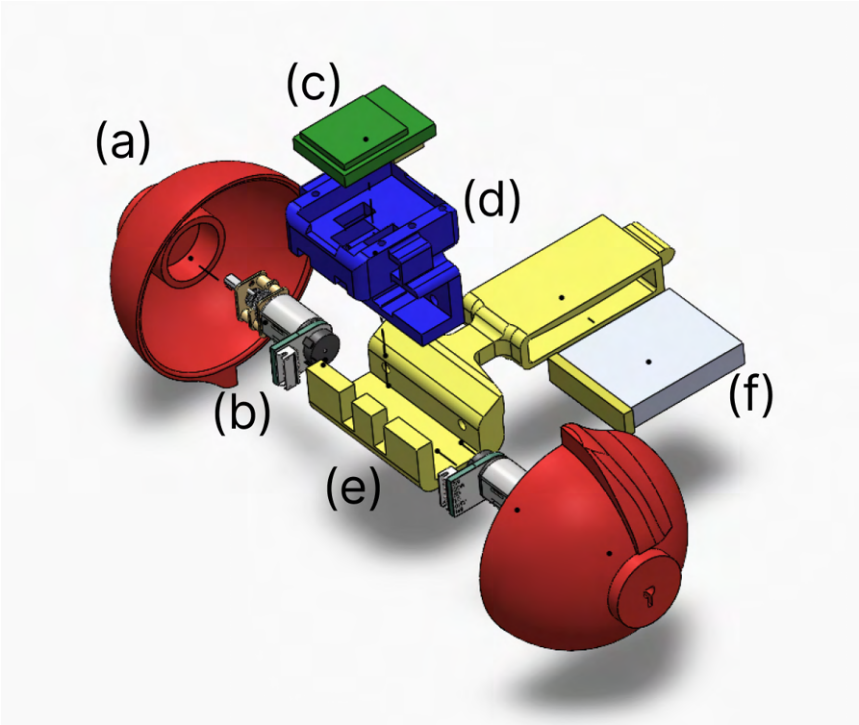

Figure 3.2: Exploded View of the Rescue Roller with Snail Cam Wheels (red), Tail (yellow), Custom PCB (green), Chassis (blue), battery (silver and yellow) and motors

Electrical Design

The RESCUE rollers use a custom PCB (See figures 3.4 and 3.4) featuring an ESP32-S3 System on a chip (SOC). The ESP32-S3 provides built-in wireless communications

Figure 3.3: The front of the RESCUE Roller's PCB contains an ESP32-S3 System on a Chip (Red), a connector for a camera breakout board (Orange) and additional through hole connections for I2C or SPI sensors (Green)

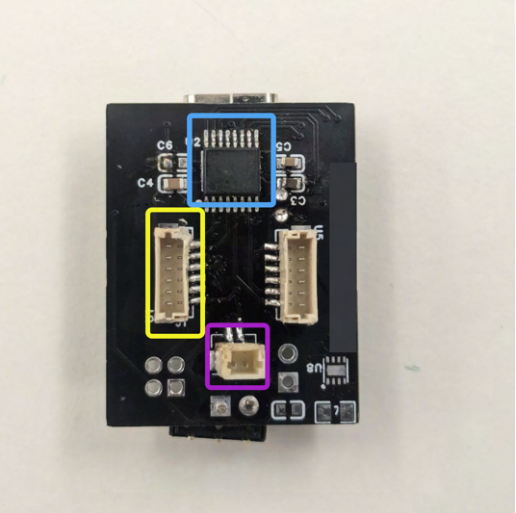

Figure 3.4: The back of the rescue roller PCB contains a DRV8833 Motor Driver (Blue), JST connectors for Pololu motors (Yellow), and a battery cable connector (Purple)

capabilities, including Bluetooth and WiFi. Additionally, the board supports interfacing with up to four serial peripheral interface (SPI) and 2 inter-integrated circuit (I2C) devices. This allows for interfacing with a wide variety of additional sensors for monitoring the robots state and the environment. While sensor selection and configuration are left for future work, the existing PCB contains the necessary scaffolding to connect additional sensors without hardware modification. Notably, it also includes a board-to-board connector for an HD camera module. The PCB also handles motor control, connecting the two drive motors to the ESP32-S3 through a DRV8833 brushed motor driver (Texas Instruments). This driver enables independent speed and direction control of each of the motors, supporting differential motion.

3.0.3 Mobility Performance Characterization

Two established characteristic dimensions for assessing traversability in search and rescue environments are verticality and obstacle severity [23]. Verticality refers to the frequency and steepness of the terrain the system must overcome, while obstacle

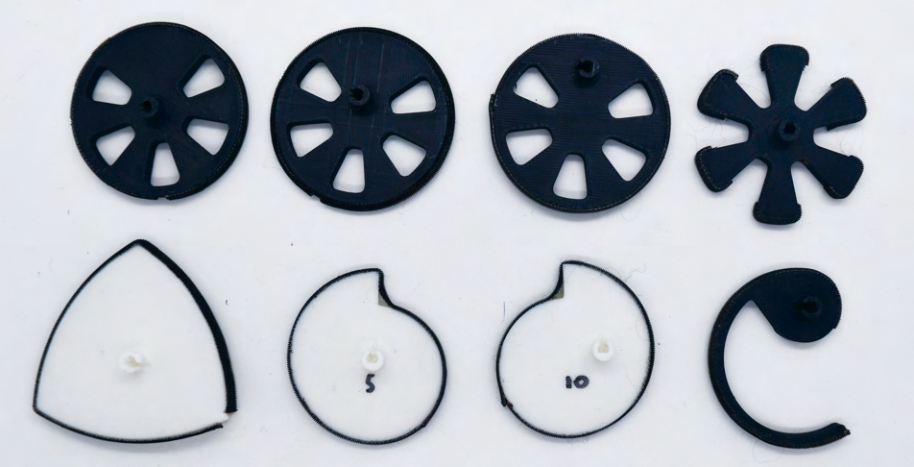

Figure 3.5: All of the test wheels - First row: Standard concentric drive wheel, a circular wheel with the drive shaft offset by 5mm (5mm eccentric), a circular wheel with the drive shaft offset by 10mm, and a spoked wheel. Second row: Reuleaux triangle wheel, a "snail cam" with a 5mm step and 5mm of eccentricity, a "snail cam" with a 5mm step and a 10mm of eccentricity, and a Rhex style "wheg" wheel.

severity references the scale of obstacles that the system can overcome. We evaluate each of these dimensions individually across eight distinct wheel designs 3.5 to understand how geometric variation impacts performance along these dimensions.

These designs draw inspiration from existing systems such as the RHex robot [26], various stair climbing mechanisms [13, 29] and the SORA-Q Lunar Rover [32].

Three of these designs are based on conventional circular wheels, with variation in eccentricity. As opposed to concentric wheels where the driveshaft is located at the geometric center, eccentric wheels are driven with an offset. We examine concentric wheels, in addition to 5mm and 10 mm eccentric variants.

The five remaining designs deviate further from traditional wheel shapes. The first is a "spoked" wheel, which omits the outer rim, relying on the open spokes to create lift surfaces that may help raise the robot over obstacles. The second is based on the Reuleaux triangle, a "curve of constant width". Although it has flat regions, rotation about its center produces motion similar to that of a circular wheel. We hypothesized that the flat edges could offer mechanical advantage when climbing. The next class of geometries we looked at where"snail cams", characterized by a spiral profile that rapidly drops to a smaller radius. Similar to the Reuleaux triangle, these

profiles were expected to provide a"step" that could increase climbing performance. Finally, we test RHex-style wheel, a well-known"wheg" or wheel-leg hybrid, design that has been used in existing research to drive all terrain robots.

To ensure consistency, the farthest point on each wheel is 25 mm from the geometric center, with the expection of the Reuleaux triangle where the furthest point is 35 mm from the center. This is a necessary adjustment to maintain an equivalent effective radius when the triangle rotates. All the wheels are 3D Printed in PLA and 3M GM400 Black Gripping Tape is adhered to the outer surface of each wheel where it would make contact with its environment to increase friction.

Verticality

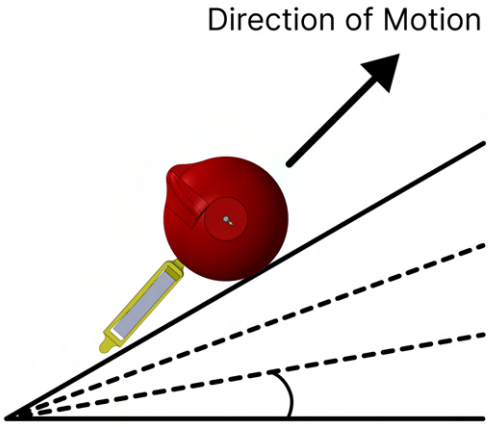

Figure 3.6: The RESCUE Roller's ascent ability was tested on slopes ranging from 10deg to 30deg, in step sizes of 10deg.

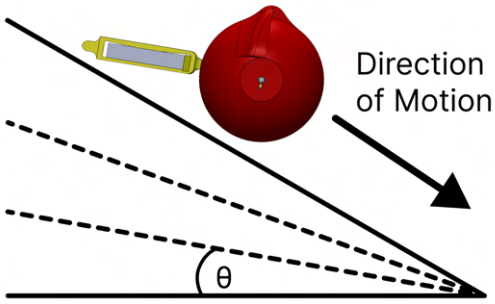

Figure 3.7: The RESCUE Roller's descent ability was tested on slopes ranging from 10deg to 30deg, in step sizes of 10deg.

To evaluate the system's capabilities in terms of verticality, we use two symmetric test setups presented in figure 3.6 and figure 3.7. Each setup consists of a large acrylic plate serving as a ramp surface, and a collection of 15 mm thick 3D-printed plates. By varying the number of plates supported by one end of the ramp we approximate slopes of 10°, 20° and 30°.

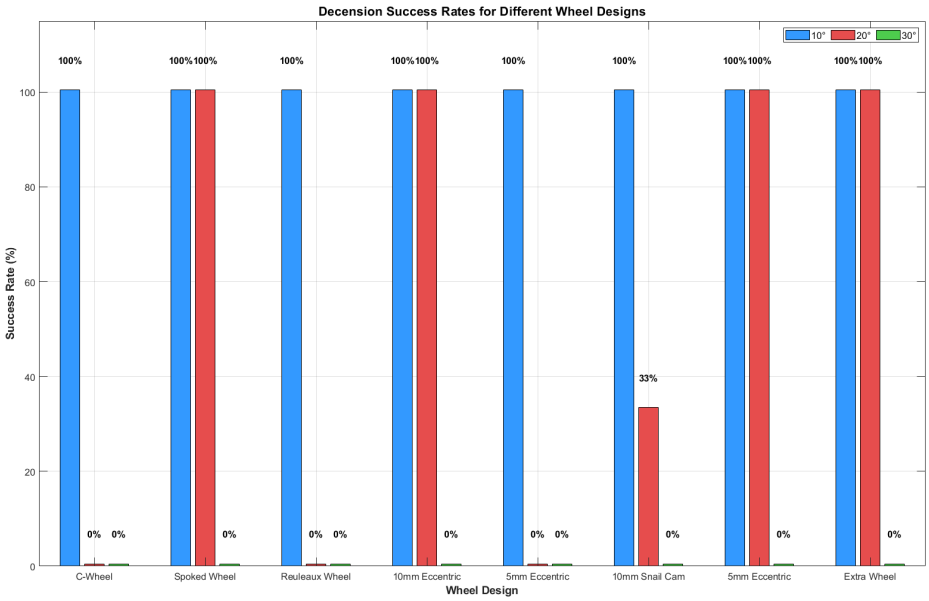

Figure 3.8: Success rates of different wheels attempting to descend slopes. All wheels successfully descend 10° slopes, however none successfully descend 30° slopes and only 5 of the 8 have any success on the 20° slope.

In each trial, the robot is placed at the base of the ramp (or top in the descent case) and released to run at full power. Each incline and wheel combination is tested 3 times. The results are coded **(S)**uccess if the robot climbs or descends the entire length, or **(F)**ailure. Results are summarized in figure 3.9 and figure 3.8.

Across both ascent and descent experiments, all wheel designs successfully traversed the 10° slope. Interestingly, the 10,mm eccentric and snail cam wheels show inconsistent success on 10° ascents but manage to complete climbs at higher angles, suggesting testing variance rather than capability. No wheel design successfully completed a 30° ascent or descent under the tested conditions.

The spoked wheel and 5,mm eccentric wheel exhibited the highest overall performance, consistently completing both ascent and descent at 10° and 20°. In contrast, the RHex-style wheel performed the worst in this evaluation. It is important to note that previous implementations of the RHex design typically use four to six actuated wheels [26], whereas our system employs only two, which likely impacts its performance.

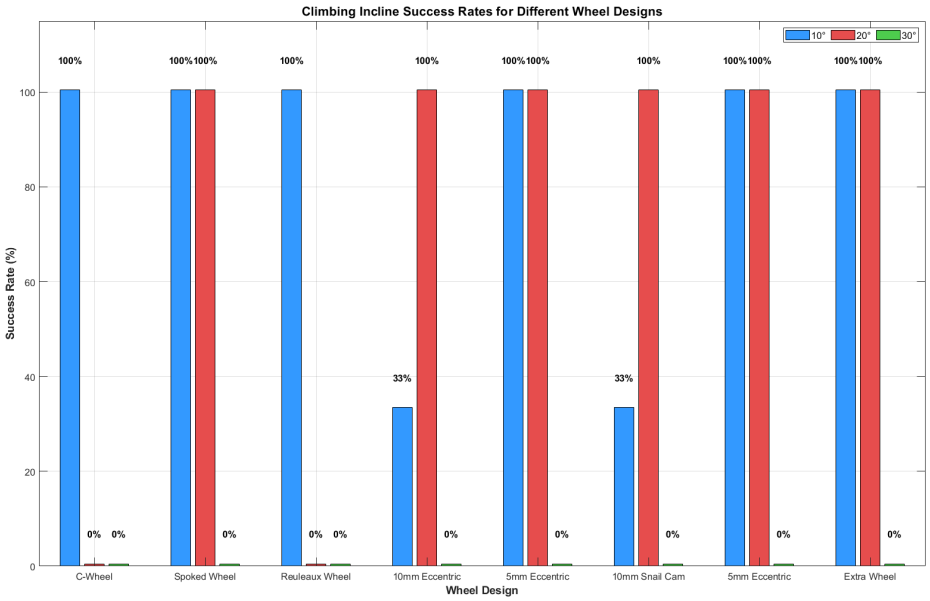

Figure 3.9: Success rates of different wheels attempting to climb slopes. All wheels successfully climb the 10° slope. None successfully climb the 30° slope and mixed results on the 20°

Obstacle Severity

To assess the system's ability to overcome positive and negative obstacles, we again use 15 mm 3D-printed plates to simulate debris, rubble, or terrain voids. Two experimental setups—shown in Figures 3.11 and 3.10—test the robot's performance over positive obstacles (raised surfaces) and negative obstacles (gaps or pits), respectively.

For positive obstacle climbing, the RESCUE roller is placed approximately 5 cm from the leading edge of the obstacle stack. We drive the robot forward at full speed and observe its ability to overcome the obstacles in two stages:

1. Mounting - classified as successful if the robot raises both wheels off of the ground and onto the obstacle
2. Surmounting - classified as successful if the robot raises its tail off the ground and onto the obstacle

The two staged approach allows us to further separate the performance of the different designs. The results of the positive obstacle evaluation are presented in

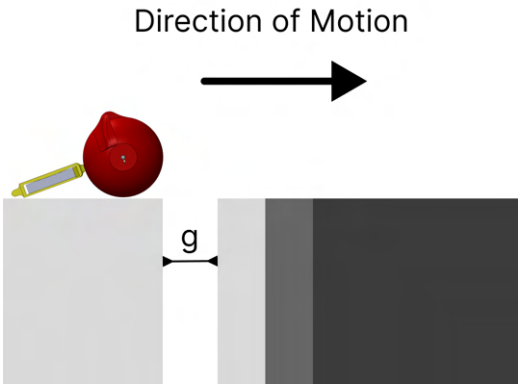

Figure 3.10: The RESCUE Roller's ability to cross gaps was evaluated on gaps ranging from 8mm or ≈10% of the body length up to 75mm or ≈90% of the body length.

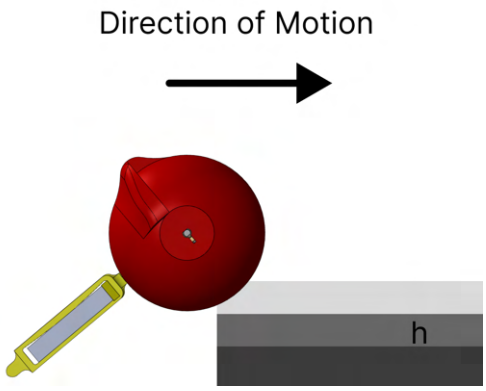

Figure 3.11: The RESCUE Roller's ability to climb over obstacles was evaluated using fixed 3D printed surfaces. All wheels were tested until failure.

figure 3.12 and figure 3.13.

The Rhex, spoked, 5 mm snail cam, and 10 mm eccentric all demonstrated equivalent success in the mounting phase, with 100% mounting rates on both 15 mm and 30 mm obstacles. In contrast, the standard wheel design fails at mounting any obstacle we tested. When we extend the evaluation to include surmounting as a subsequent state, we clearer distinctions emerge. Only the Rhex and spoked wheel are fully successful at climbing 15 mm obstacles. The 10 mm eccentric and 10 mm snail cam are the only wheels that are successful at surmounting the 15 mm obstacle. The 30 mm obstacle proved too much of a channel for any of our designs to surmount, suggesting an upper bound for these configuration.

For negative obstacles, we tested gaps ranging from 8 mm to 75 mm. No wheel design consistently crosses a gap larger than 40 mm and once we reach 50 mm we see no successful crossings. Most wheel designs begin to drop performance at 25 mm, however the 5 mm eccentric wheel manages to succeed in all trials for a 40 mm gap. The best performing designs in this evaluation were the 5 mm snail cam and the standard wheel, which maintained relatively high performance on the 40 mm

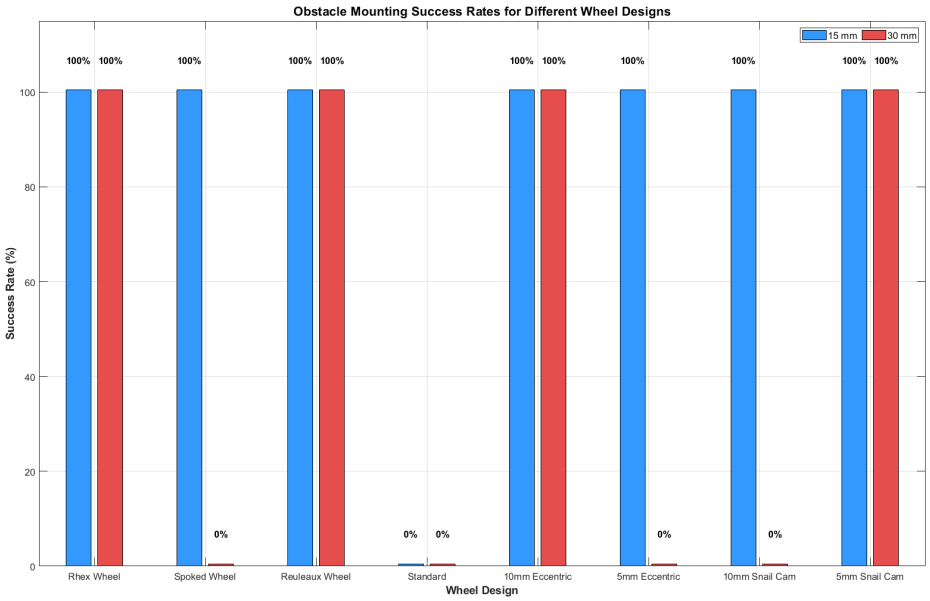

Figure 3.12: Obstacle climbing success rates across gaps ranging from 8mm to 50mm. No configuration successfully managed to cross gaps exceeding 40mm, although values up to 75 mm where tested.

obstacle.

3.0.4 Characterizing RESCUE Roller Force Application

To evaluate a RESCUE Roller's ability to steer the Vine Robot, we first establish the push and pull forces the RESCUE Roller can apply on different surfaces. To assess the pulling force we used a 0-500g force transducer (Precision Gram Load Cell, Transducer Techniques) with one side fixed to an upright surface and the other side attached to the robot with a fishing line loop (Figure 3.15 (a)). The pushing force of was measured in a similar manner, but with the transducer attached to the RESCUE roller's chassis, and the robot driven towards the upright surface (Figure 3.15(b)). These tests were performed on surfaces of varying friction, compliance, and roughness, including: an acrylic sheet, medium density fiberboard (MDF) with a Life-Grip Anti Slip Tape on, MDF without the tape, a 3D printed rough or rocky surface (variance of 3mm [**?**]), and an artificial turf of uniformly distributed 1 inch long plastic strips.

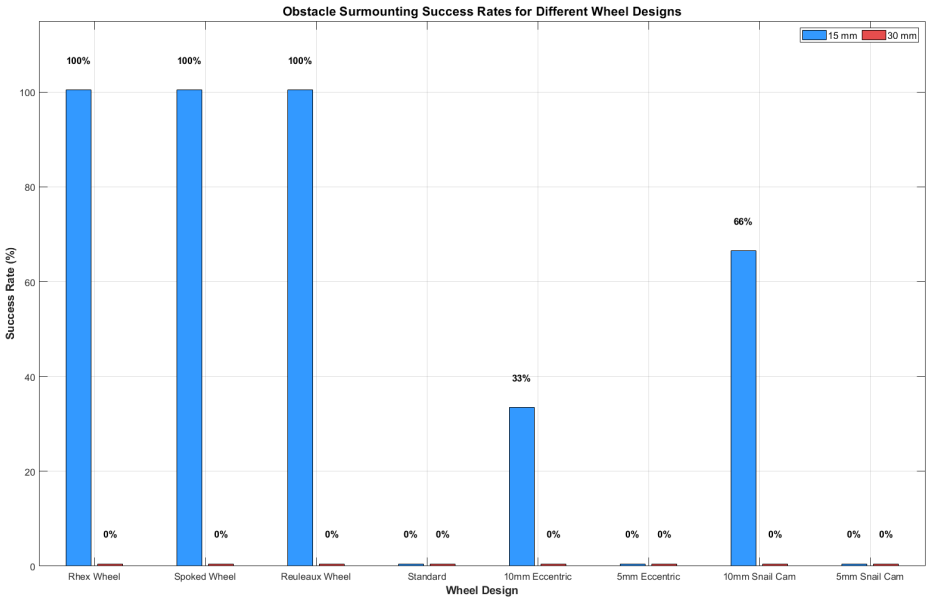

Figure 3.13: Obstacle mounting success rates across gaps ranging from 8mm to 50mm. No configuration successfully managed to cross gaps exceeding 40mm, although values up to 75 mm where tested.

Images of the terrains are available in A. In both evaluations, we collected data for 10 seconds. The results are tabulated in Figure **??**. Larger presentations of the figures are available in A.

Our analysis shows that across our material and wheel suite, pulling results in higher average forces than pushing, with averages of 0.22 N and 0.1 N respectively. We treat this as our prefered direction of steering. Evaluating the relative wheel performance, we see the highest force with the spoked wheel with an average of 0.253 N. Notably, the performance for the concentric, and both cam wheels result in forces within 0.01 N of the spoked wheel.

Based on the cumulative results of our mobility and force experiments we select the snail cam as our final geometry. It demonstrates high performance across the board on slopes, obstacles, and force exchange. In our tests we see an average pulling force of 0.245 N and a maximum of 0.29 N on the artificial rocky surface and MDF with tape (3.17. It also avoids potential issues with the spoked wheel if debris is caught between the spokes.

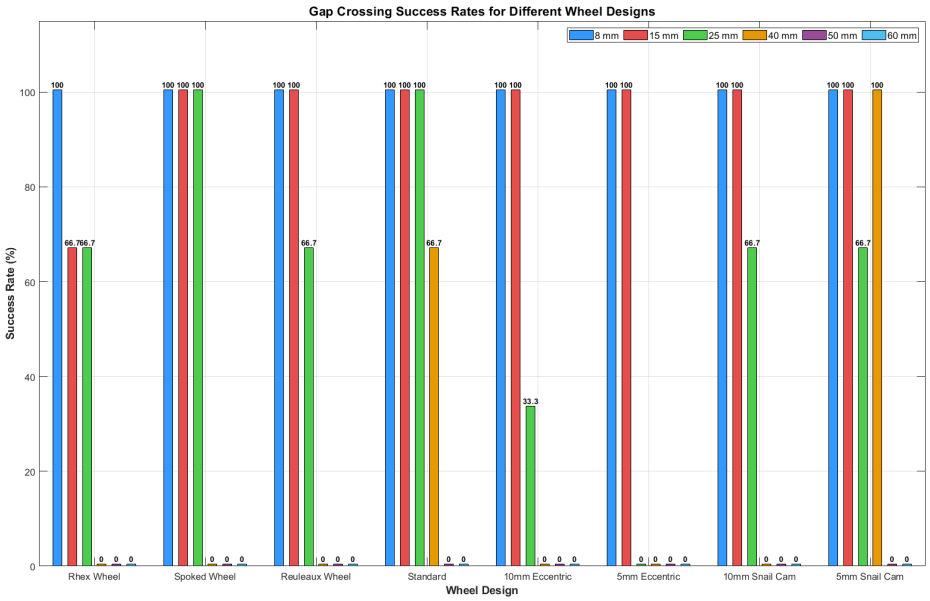

Figure 3.14: Gap crossing success rates across gaps ranging from 8mm to 50mm. No configuration successfully managed to cross gaps exceeding 40mm, although values up to 75 mm where tested.

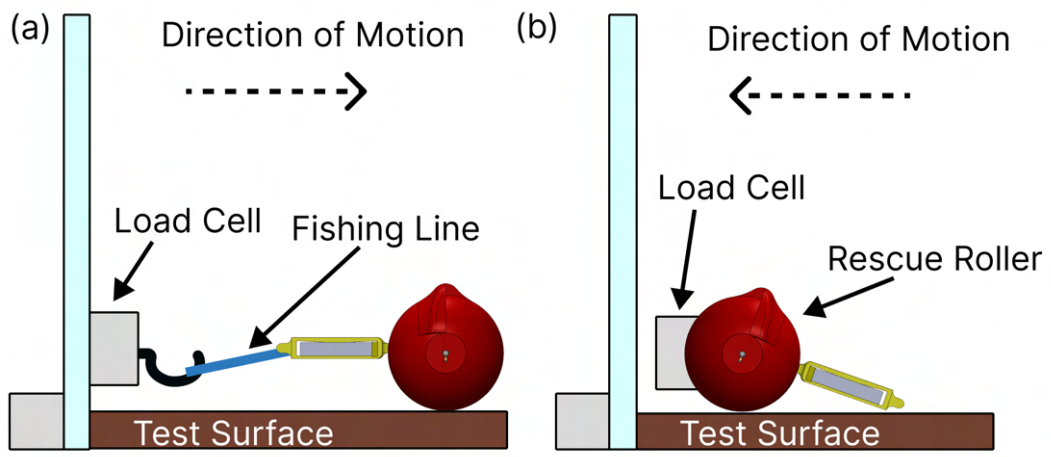

Figure 3.15: RESCUE Roller (a) pulling and (b) pushing force experimental setups. The experiments were performed on five test surfaces with different friction, compliance, and roughness.

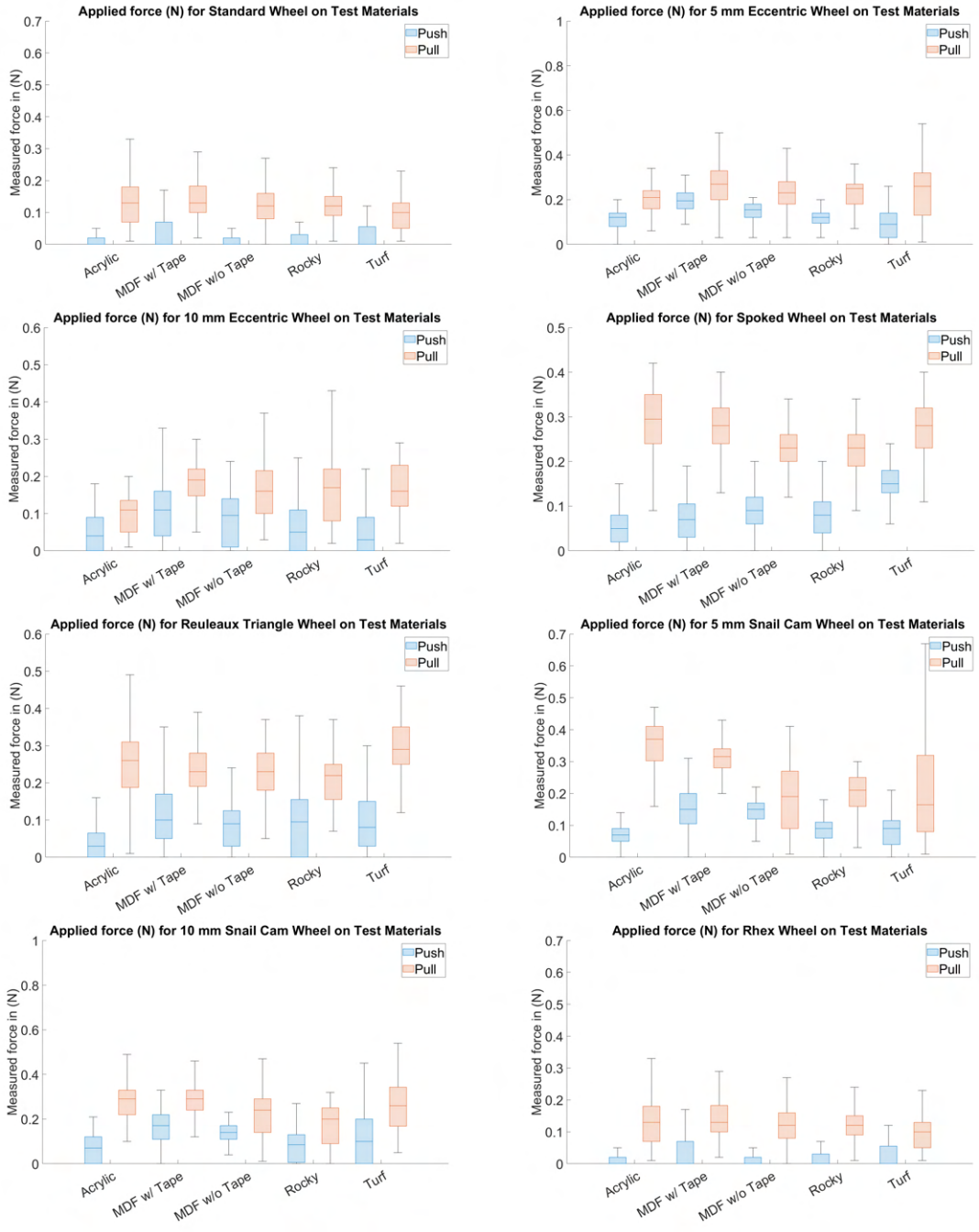

Figure 3.16: Force application results for each of the eight wheels on each of our five test surfaces.

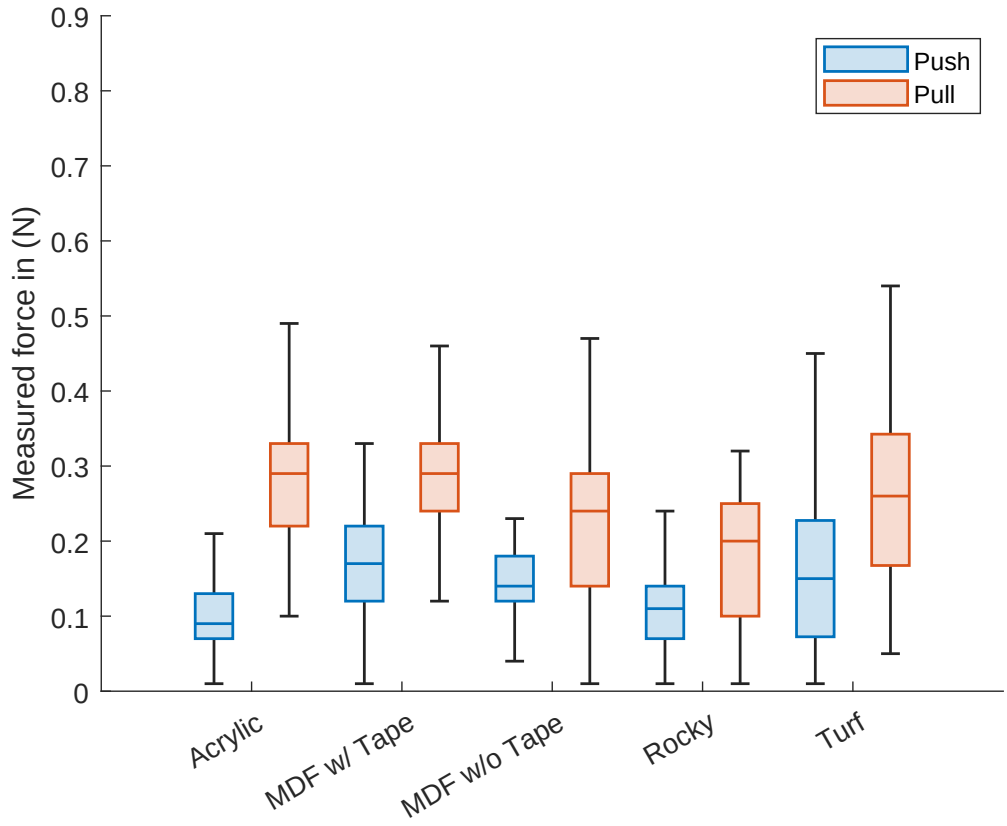

Figure 3.17: Applied force on acrylic, medium density fiber board (MDF), MDF surfaced with Life Grip Tape, an artificial rocky terrain, and artificial turf by a RESCUE Roller robot with 10mm step snail cam wheels.

We successfully deploy the RESCUE roller Ant outside laboratory settings, Figure 3.18, validating the ability of the selected wheel geometry to locomote in unstructured, high-variance terrain.

3.0.5 Vine Robot and RESCUE Rollers collaboration:

Finally, we demonstrate the combined Deployment-Capable Vine Robot and RESCUE Roller team to showcase the full collaborative movement capabilities in a single scenario. The demonstration is carried out on a course that includes a ramp and a platform, as shown in Fig. 3.19. In the demonstration, the Vine Robot extends with one RESCUE Roller inside for 35 seconds (Fig. 3.20(a)). At 79 seconds, Fig. 3.20(b) shows the first RESCUE Roller successfully deployed, while tethered to the Vine

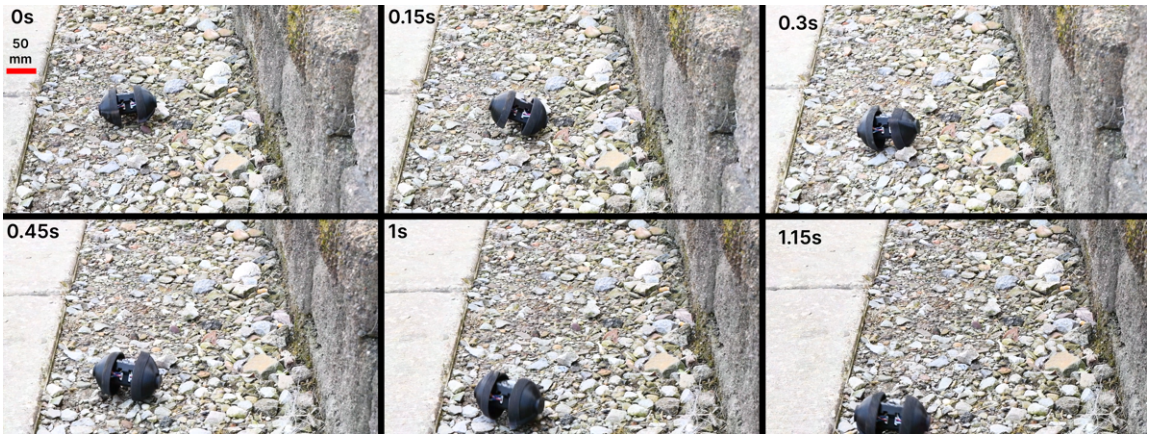

Figure 3.18: We allow a RESCUE roller ant to freely move on uneven rocky terrain outdoors. The positions in intervals of 0.15s are presented demonstrating the continuous motion of the robot and its ability to perform in the presence of highly variant terrain.

Robot by a string. It then moves from right to left, steering the Vine Robot to face the incline opening, stopping at 110 seconds. Next, a second RESCUE Roller is inserted to be carried by the Vine Robot, and the Vine Robot grows up a 30-degree incline (Fig. 3.20(c)). Finally, the Vine Robot deploys the second RESCUE Roller atop the incline (237 seconds), and the RESCUE Roller can drive around on the surface (Fig. 3.20(d)).

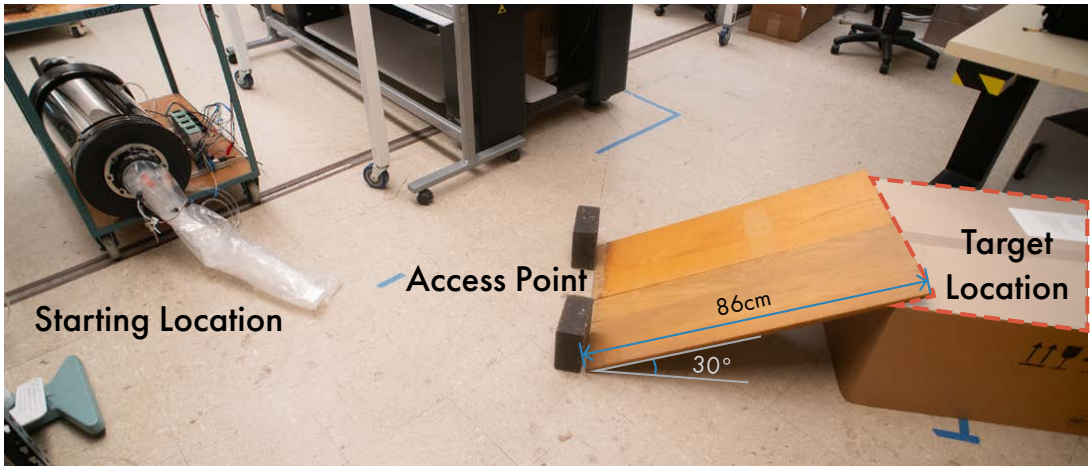

Figure 3.19: Experiment Setup to demonstrate the concept of heterogeneous collaboration. The Vine Robot will carry a RESCUE Roller to the target location,which the roller is normally unable to reach due to a ramp with 30° angle.

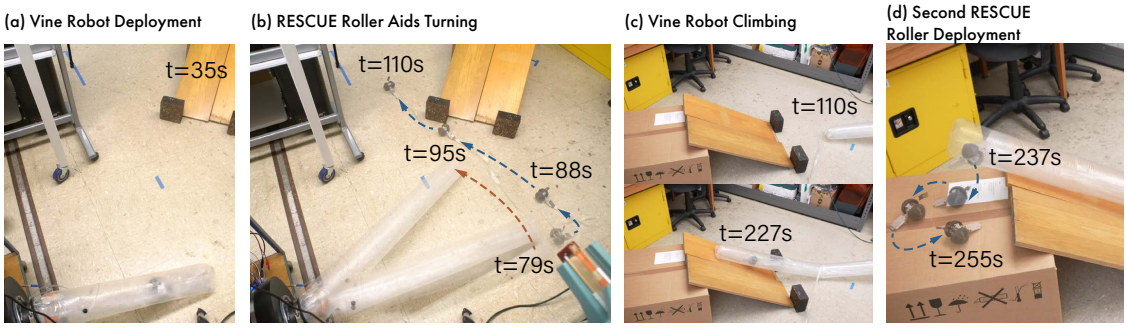

Figure 3.20: Demonstrating the Deployment-Capable Vine Robot deploying multiple RESCUE Rollers and the RESCUE Rollers helping the Vine Robot to steer. (a) The Vine Robot starts to grow with a RESCUE Roller to deploy already inside the growing body. (b) The Vine Robot deploys the first RESCUE Roller, which is tethered to the robot. The RESCUE Roller then pulls the Vine Robot to steer it towards the ramp where it then (c) grows up the ramp to carry the second RESCUE Roller atop the platform and (d) finally, deploy the second RESCUE Roller in the target area.

Chapter 4

RESCUE Roller Beetle

4.1 Overview

Building on our experiments with the RESCUE Roller Ant we introduce several modifications to the platform for the next iteration. First, we include a Long Range or LoRa radio chip for communication while deployed. We also modify the drivetrain to reduce the footprint and improve deployment, specifically enhancing deployment via the vine robot, while retaining a high degree of independent mobility. Finally, we apply the philosophy of modular and reconfigurable robots to improve performance on inclines and over obstacles, simultaneously improving data communication between rollers.

The intent of modular and reconfigurable robotics, is to enable robots to adapt to their environment, helping to maintain task performance in dynamic conditions. The fundamental elements of an MRR are the module, or the individual pieces that make up the system, and the linkage, which allows the modules to interact. Researchers have proposed various mechanisms for robustly connecting multiple robots, including compliant physical structures [36], permanent and electromagnets [5, 17, 21], and motorized hooks [35]. In many systems, components do not communicate through their physical connections. However, [16] demonstrates a system where components exchange limited information with adjacent neighbors via infrared light to determine their state and coordinate reconfiguration.

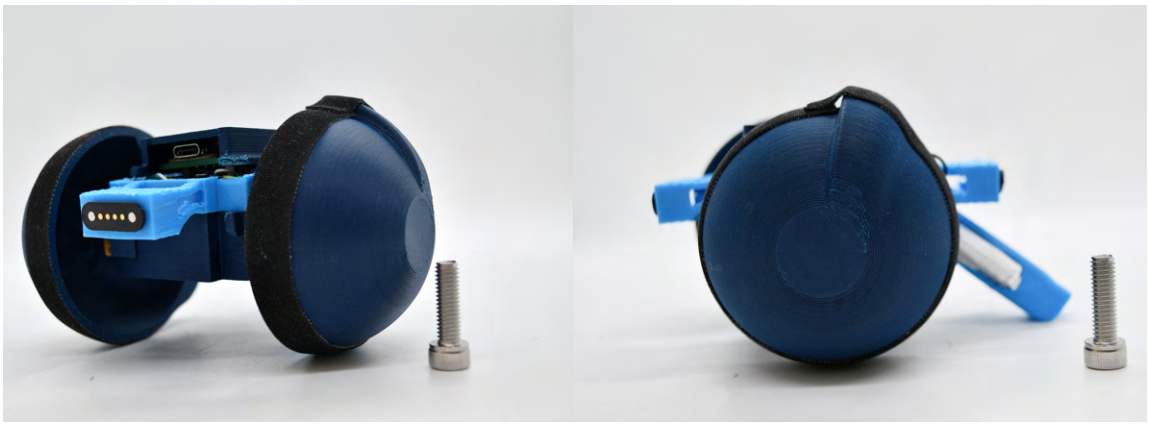

Figure 4.1: A fully assembled RESCUE roller from the front (left) and side (right). The tail monobody (light blue), is fabricated from thermal polyurethane (TPU) tail. The chassis and wheels (dark blue) are fabricated from polylactic acid (PLA). All parts where printed using a Bambu Labs X1. The systems battery and the magnetic connectors are featured in the tail. An M6 20mm bolt is included for scale.

4.2 Mechanical Design

We use an identical actuator and wheel geometry to the Ant, namely differential drive with two Pololu 250:1 Gear motors, that are housed in the chassis in addition to a custom PCB. We retain a PLA chassis and include the stabilizing tail housing an identical battery. We modify the tail to house magnetic connectors detailed in Figures 4.2 and 4.3. We transition from PLA to thermal polyurethane (TPU) for the tail taking advantage of the robustness of TPU and providing compliance for the connectors. The wheels are 65mm hemispheres with one side flattened to support 3D printing. The wheels include a 10% (6mm) step functioning as a support to improve obstacle climbing. 3M GM400 Black Gripping Tape is adhered to the outer surface of each wheel where it would make contact with its environment to increase friction.

4.3 Electrical Design

We develop a new custom PCB for the RESCUE Roller Beetle featuring the same ESP32-S3 System on a chip, and DRV8833 brushed motor driver (Texas Instruments). We also include an Adafruit RFM95w module to allow for Long Range (LoRa) radio

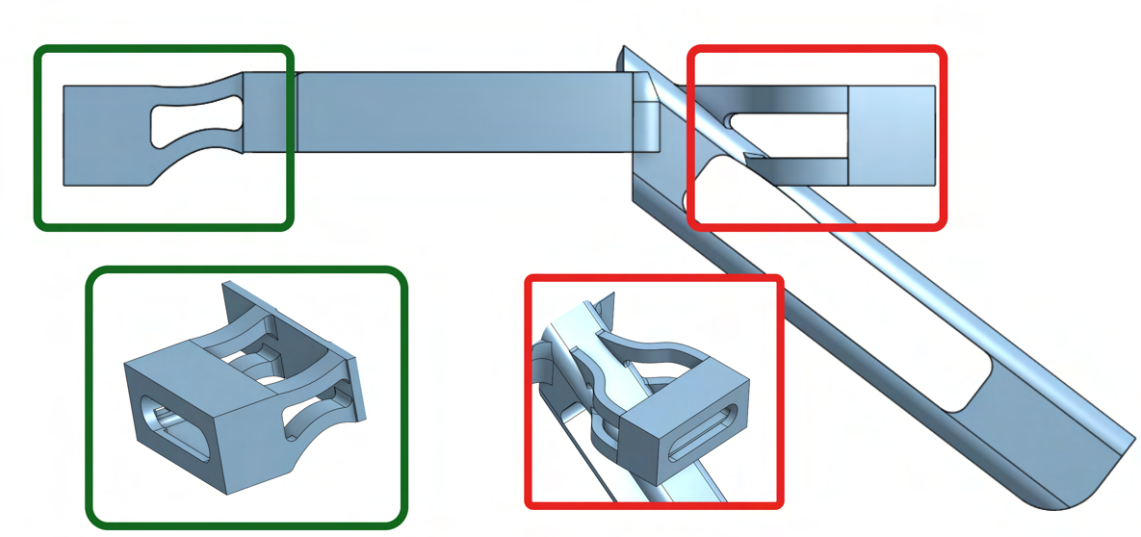

Figure 4.2: CAD rendering of the inner layer of the RESCUE roller. The entire structure is fabriated from thermal polyurethane (TPU) with the front (red) and rear(green) connectors having distinct designs. The front geometry results in a more rigid fixture for the magnetic connector, while the rear is more compliant to yaw and planar variations. The combination allows the system to successfully dock and disconnect without requiring powerful actuators.

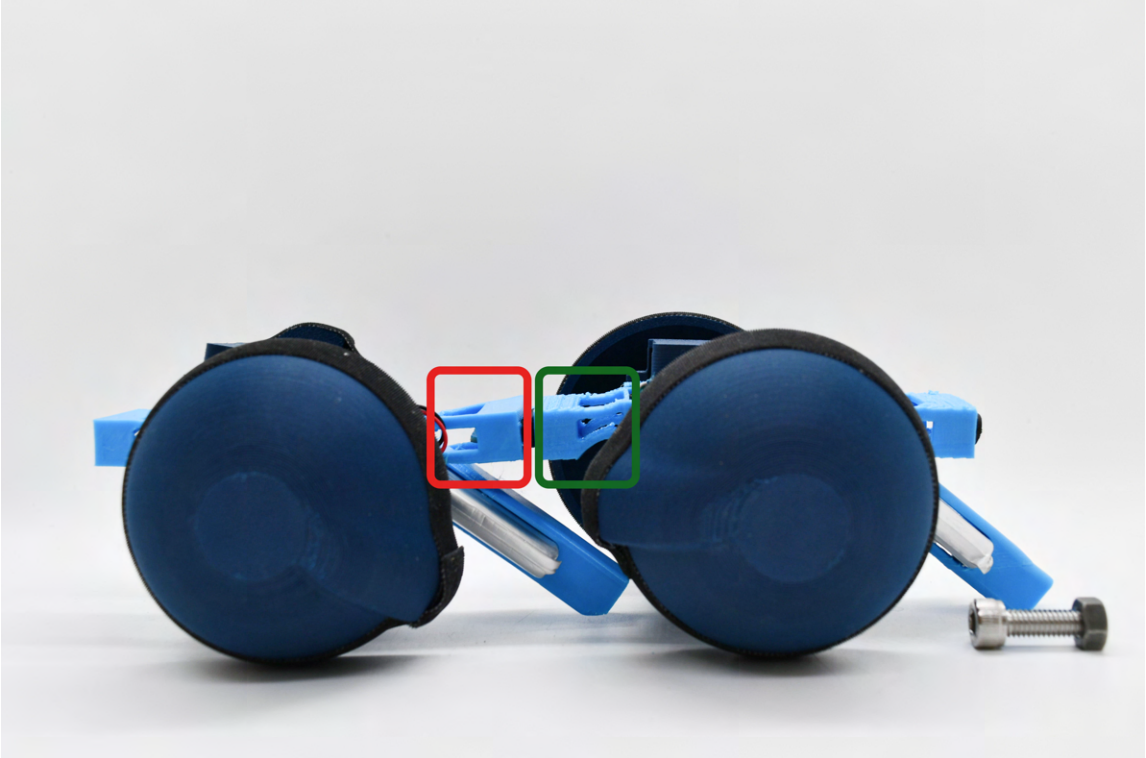

Figure 4.3: Photograph of two RESCUE rollers connected using the magnetic connector. The front connector (green) of the right most RESCUE roller is connected to the rear connector (red) of the left most RESCUE roller. The compliant TPU is printed in a light blue filament, in contrast to the rigid PLA components in the dark blue.

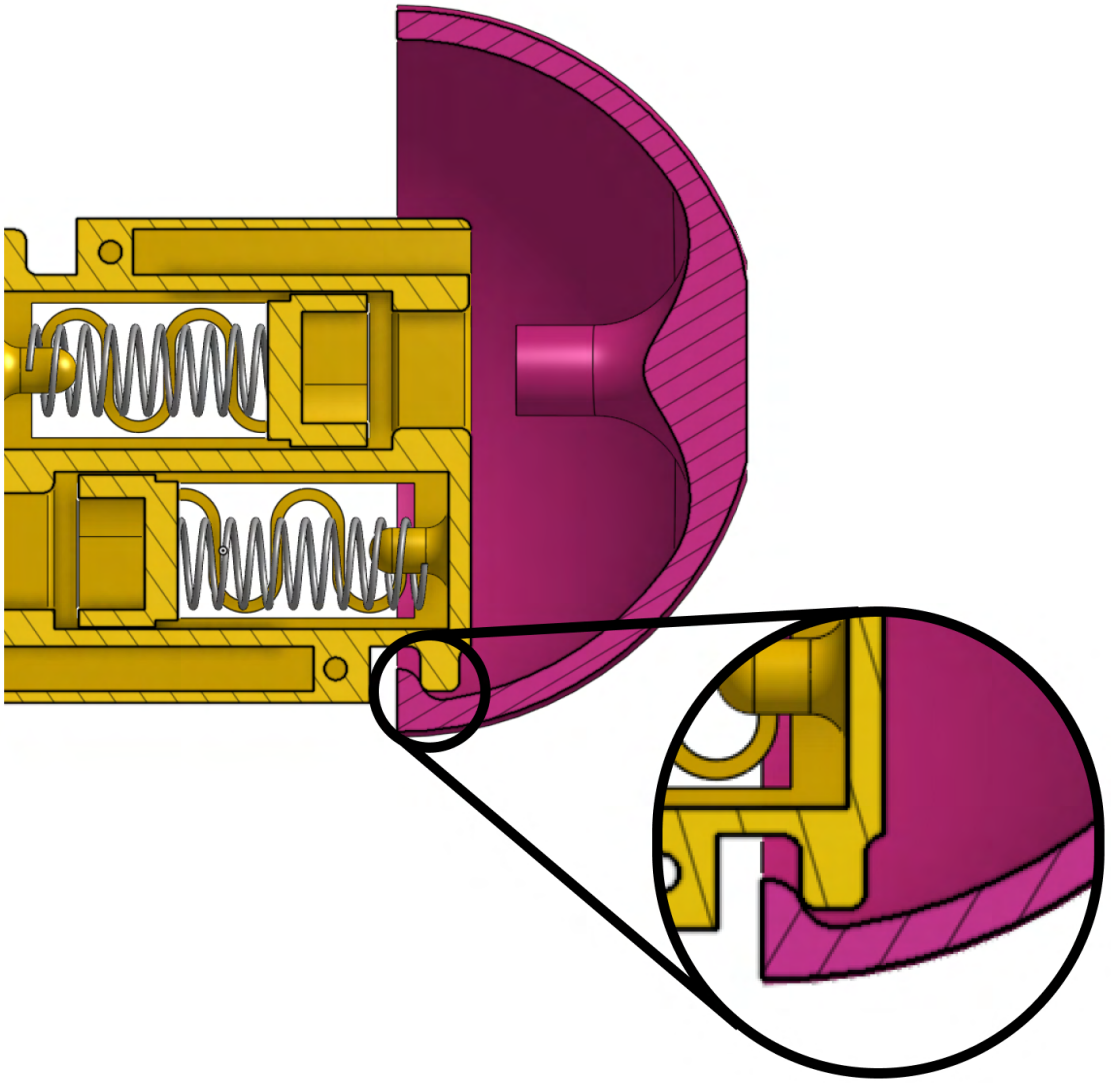

Figure 4.4: Cutaway of the chassis (yellow) and a wheel (pink) of the modified RESCUE roller. The chassis retention clip and corresponding protrusion on the wheel hold the wheel shut when the robot is secured. By rotating the wheel, the two clips come out of alignment and the system passively expands to the full wheelbase. The wheelbase expansion mechanism uses PLA to print a housing for the Pololu gear motors. An additional metal spring is placed in parallel with a printed one to enhance energy storage and limit the impact of material fatigue in the PLA

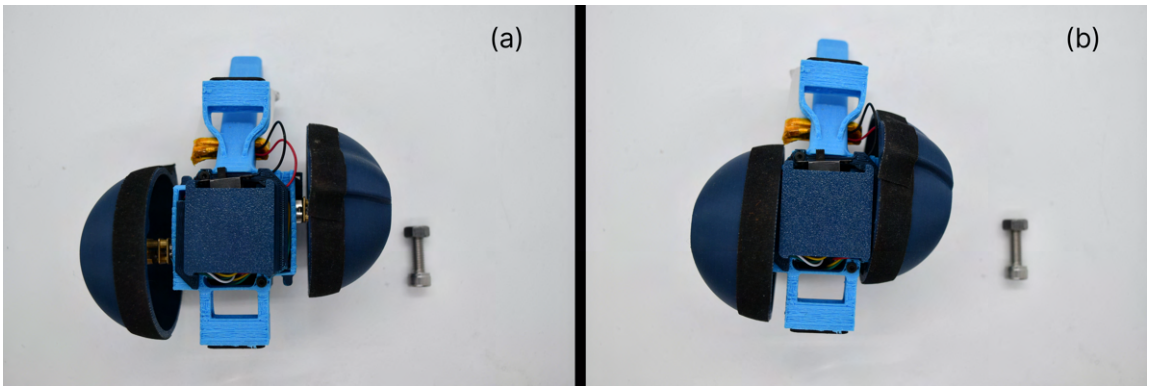

Figure 4.5: The robot's drivetrain starts compressed (a) and locked in place. In this configuration the distance from wheel to wheel is approximately 68 mm. When the wheels rotate springs provide a force to expand the wheelbase (b). When fully expanded the wheelbase measures approximately 84 mm. An M6 20mm bolt is included for scale.

communication and a BNO085 9-axis inertial measurement unit. We believe this unit could be used to improve odometry and assist with aligning the connectors.

4.4 Wheelbase Adjustment

Regardless of system capabilities, a robot must be successfully deployed to provide operational value. In urban search and rescue (USAR) scenarios, chaotic and unpredictable conditions often eliminate the possibility of predefined entry points. Using a centimeter-scale systems increases the likelihood that robots can exploit naturally occurring voids for access. Although responders are equipped with tools to create access points manually, smaller robots reduce the number and size of required openings, significantly decreasing deployment time.

In our initial work we explored vine robots as a deployment mechanism for micro-robots. Owing to their inflatable design, vine robots can passively deform and navigate confined environments [4, 12]. However, the rigid chassis of the RESCUE roller constrains the minimum opening size that the vine robot can enter. Further size reduction of the Ant would mitigate the constraint the micro-robot applies. However, debris and obstacles in the environment can introduce large roll angles for the system. These could occur from driving on inclined planes formed by falling

debris, or driving over obstacles that only disturb one wheel. If the robot overturns, mobility performance will be dramatically reduced.

The system will tip over when the experienced roll angle exceeds θ_{tip}, which is equivalent to

$$\theta_{tip} = tan^{-1}(W/2h_{cg})$$

where W is the wheelbase of the system and h_{cg} is the height of the center of gravity [24]. Consequently, the roll angle of our system is proportional to the wheel separation.

To take advantage of a smaller footprint while being carried, and allow a wider more stable configuration while locomoting, we design our chassis to allow the wheelbase to adjust. Rather than utilizing a coaxial drivetrain setup, we stack the actuators front and back to allow space for motion. We place the motors within housings with both compliant springs fabricated from FDM printed PLA and steel springs [1]. The compliant spring and housing restrict the motion of the motor to be linear, while the steel spring stores the energy used for displacement. The chassis can be held in its compressed state by aligning clips on the interior of the wheel with corresponding clips on the chassis. This maintains the small form factor prior to deployment while allowing the robot to extend to the full wheelbase without needing an additional actuator (Figure 4.4).

Our design is capable of 16 mm of compression transitioning from 84 mm to 68 mm (Figure 4.5) a reduction in size of $\approx$ 24%. With an approximate h_{cg} of 36 mm, this corresponds with a theoretical roll angle change from 29 to 42 degrees, an increase of 44%. We show the robot successfully remaining stable on a 40° slope in Figure 4.6.

By allowing the wheelbase to expand we can take advantage of the stability of a larger base, while capitalizing on the small footprint during deployment.

4.5 Physical Connection

To further enhance mobility and task performance, the RESCUE Roller robots are designed to form local pairings through physical connection, enabling collaborative behavior. We build upon the Ant's chassis design, modifying it to support modular linking between units. Specifically, we integrate mounts for Adafruit 4-pin magnetic

Figure 4.6: RESCUE roller on a 40 degree slope. With the adjustable wheel base we have a larger roll angle than in a fixed, small chassis case.

connectors [7] at both the front and rear of each robot's tail. The new tail is constructed from thermoplastic polyurethane (TPU), which introduces compliance to accommodate misalignment during docking maneuvers and variance during motion.

The magnetic connectors exhibit their greatest holding force in the axial direction, while their grip weakens significantly under shear. We exploit this directional property to enable smooth disconnection through counter-rotation. By rotating paired robots in opposite directions, the magnets separate without requiring large torques, allowing continued use of compact actuators and weaker magnets that minimize unintended interactions with the environment.

Beyond mechanical coupling, the magnetic connectors also support inter-robot communication and power sharing. The four pins are assigned to TX, RX, GND, and 5V, respectively. We implement UART (Universal Asynchronous Receiver-Transmitter) for initial communication, though the system is designed to be compatible with CAN-bus or other custom protocols to support larger robot chains. This communication

Transmission Method	Spreading Factor/Baud rate	bits/second
LoRa	12	57.03
LoRa	7	1.58e3
UART	9600	3.71e6
UART	115200	3.8e6

Table 4.1: The results of our data transmission tests are reported. We operate at a fixed frequency of 525 MHz for both our tests using LoRa and vary our spreading factor between 12 (max) and 7 (minimum). For UART we evaluate transmission rates at baud rates of 9600 and 115200. We observe a more than 1000 fold increase in bit rates between when using either UART configuration and the fastest LoRa communication achieved.

framework enables synchronized planning and information sharing within localized groups of RESCUE Rollers.

Although long-range communication via LoRa radio is available, it trades bandwidth for range, making it less suitable for close-range coordination. High-frequency coordination over radio also increases the likelihood of signal collisions, which occur when multiple transmissions interfere on the same frequency, resulting in data loss or corruption. A physical data link mitigates these issues by supporting higher bandwidth and eliminating collisions. It also ensures that locally relevant messages remain confined to appropriate agents, reducing processing overhead and the risk of erroneous behaviors. Finally, the selected full-duplex protocol allows simultaneous bidirectional communication, enhancing responsiveness and efficiency during collaborative tasks.

To validate the advantages of physical communication we compare the data rates of LoRa using two different spreading factors and wired communication. Spreading factor corresponds to the ability of the signal to cross large distances, with a larger spreading factor slowing data rate in exchange for distance and robustness. We allocate 1024 bytes of random data, and transmit it using our LoRa and UART with two different baud rates 25 times. The average speed results are recorded in Table 4.1. We see a multiple order of magnitude difference between the highest transmission speed found available from our LoRa module and both UART configurations. The ESP32-S3 does have the capability to wirelessly communicate using Bluetooth Low-Energy (BLE), Wi-Fi or ESP-NOW, however, these all expend large amounts of energy [10].

Our future work proposes utilizing the local data rates to share information between two agents for local analysis before being fed to a centralized server or repository for first responders. We also examine using the low latency communication to coordinate actions between the two agents allowing them to function as a single system rather than two proximal, yet independent, systems. We can additionally utilize the fixed connection to improve localization accuracy by combining known local transformations with existing estimates.

4.6 Performance Validation

Both the two-wheeled single Rescue Roller and the coupled four wheeled system offer improvements under different operative domains. We specifically examine maneuverability, inclines, and obstacle surmounting to demonstrate the performance benefits of attaching the secondary system, while additionally showing that constructing a fixed four-wheel system results in diminished performance in subsections of our operative domain.

Maneuverability

Without an additional actuator or degree of freedom between the two vehicles, the joint system functions as a skid steer vehicle. As a result its ability to rotate is diminished. Additionally, the skid steer system requires twice as much free space of 0.045 m^2 or a 240 mm diameter circle whereas the single system requires only 120 mm due to differing kinematics and center of rotation. In turn this results in a 75% decrease in required free space.

4.6.1 Inclines

We examine inclines as they exist as pitch changes of the terrain. We place a single RESCUE roller at the base of an inclined sheet of medium density fiberboard (MDF) fixed at one end using tape and supported to reach a prescribed slope angle. Running at full speed we allow the RESCUE roller to attempt to climb the slope. Our experiments (Fig. 4.7) show a maximum climb angle for a single RESCUE roller of approximately 28°. Similarly, we place a joined pair of rollers at the bottom of an

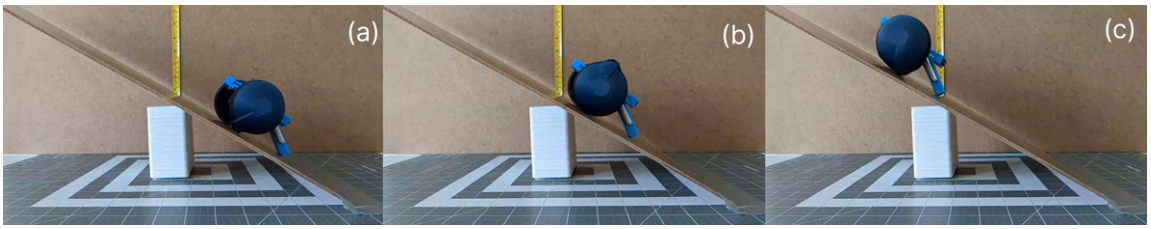

Figure 4.7: A Single RESCUE roller climbing an ≈ 28° slope initially (a), after one second (b), and after two seconds (c).

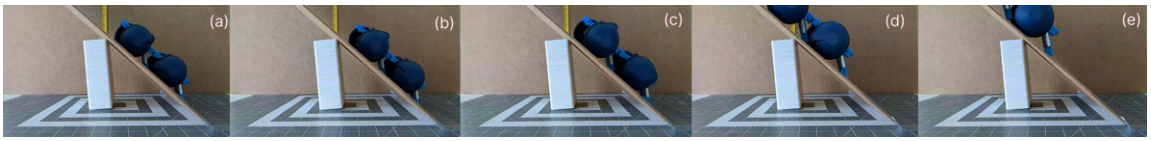

Figure 4.8: A coupled set of two RESCUE rollers climbing an ≈ 39° slope initially (a), after one second (b), after two seconds (c), after three seconds (d), and after four seconds (e)

incline and evaluate the maximum climbable incline when they operate at top speed. We see an increase of 40% raising the climbing angle to ≈ 39° (Fig. 4.8).

4.6.2 Obstacle Surmounting

To evaluate the ability of the RESCUE roller to climb obstacles. We utilize standardized PLA printed plates with a height of 5mm a depth of 50 mm, and a length of 100mm, to evaluate the upper limit of traversable obstacles. Starting with a single plate we place the RESCUE roller 75 mm from the leading edge and release them operating at full speed. Successful surmounting requires that the system can climb to the top face of the stack of plates, cross and descend from the elevated height without overturning. The maximal successful obstacles are presented in Fig. 4.9 and Fig. 4.10. We observe a 33% increase in maximum obstacle height from 30mm to 40mm when adding the additional RESCUE roller system. Leveraging the data transmission enabled by the coupling mechanism we can coordinate the motion of the two systems to approach the obstacle and detect when the initial system has climbed the obstacle using the interruption in data transmission. This allows the supporting robot to continue other task objectives.

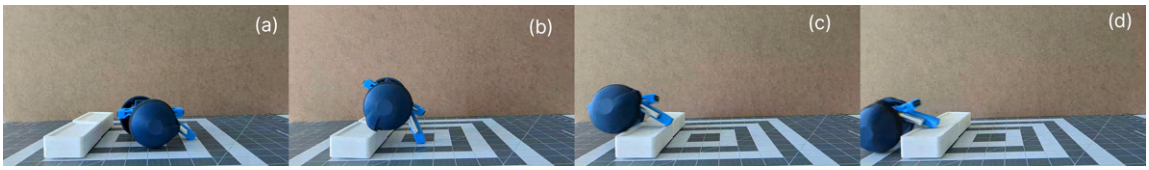

Figure 4.9: A single RESCUE roller surmounting a 30 mm obstacle. The robot approaches (a), pulls it self onto the top face (b), crosses the face (c), and descends (d) while maintaining stability and not overturning.

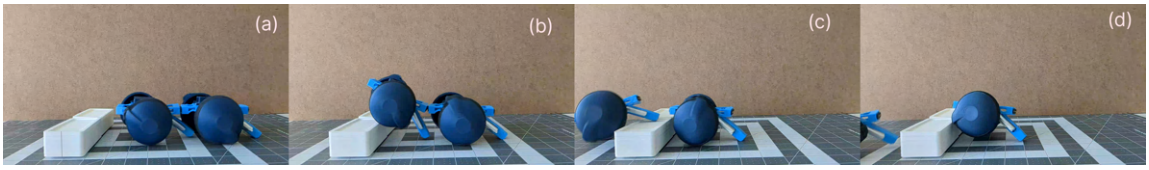

Figure 4.10: A paired RESCUE roller system surmounts a 40 mm obstacle. The additional thrust from the rear RESCUE roller allows the front system to cross a larger obstacle while it remains on the original side for further exploration. The coupled system approaches the obstacle (a), the leading robot climbs the front edge (b), crosses the top face (c) and descends (d) while the rear robot stays behind.

Chapter 5

Conclusions

In this work we take steps to improve the mobility of small robots for search and rescue. We presented the design of the RESCUE Roller Ant and resulting collaborative behaviors of the Deployment-Capable Vine Robot and RESCUE Roller. These robots complement each other's capabilities and combining them allows delivery of the RESCUE Rollers to previously inaccessible locations, and more extreme steering of the Vine Robot. By leveraging the individual skills of disparate systems to work towards a single common task, we can accomplish objectives outside the capabilities of each robot. Both multi-agent teaming, and MRR based approaches can extend the capabilities of resource constrained robots. We explore modularity and reconfiguration with the RESCUE Roller Beetle. By augmenting the original design we improved deployment and enable interactivity between RESCUE roller pairs. The Beetle's interconnections improve the mobility characteristics of the 2-bot configuration when climbing slopes and surmounting obstacles increasing performance by 40% and 33% respectively. However, maneuverability is still superior in the single robot configuration, requiring a 50% smaller footprint and enabling much more dynamic behavior. The selective reconfiguration allows the robot to take the form that best addresses its current needs.

By increasing the mobility and maintaining low cost we can create a large number of highly-mobile robots increasing the joint systems ability to complete tasks [11]. The collaborative approach we demonstrate offers a cost-effective and efficient method for deploying multiple robots in search and rescue operations for distributed exploration

and sensing. This demonstrated collaborative design does not represent the full possibilities; the Vine Robot, for example, could be used to deliver power to other robots or essential supplies to victims, while the RESCUE Rollers could be diversified and specialized through varying mapping, communication, and sensing capabilities. Physical collaborative behavior among heterogeneous robots opens new pathways for researchers and engineers to think about robot-robot collaboration for search and rescue operations.

This work opens additional avenues for exploration and leveraging the high throughput communication of the Beetle. For instance, it may prove beneficial to seek out and couple with robots to transmit large amounts of data rather than send it over the slower LoRa radio. This adds an additional consideration to the planning and optimization process for system deployment. Additionally, the specifics of the physical linkage between pairs of RESCUE rollers can be further analyzed. The current design is limited in its ability to handle elevation changes between the rollers, in addition to yaw variation. Redesigns could allow for new steering abilities similar to articulated vehicles, a modality that is only possible with strong coordination which our connectors allow. Extending the link to encompass a tether between the two rovers could allow for persistent data and power sharing, or allow one robot to"belay" another down treacherous drops. We are also exploring specializing the operations of the RESCUE rollers. Robots designed to serve as the rear in a link of rollers might be designed with higher torque actuators while the front has a reduced mass. Creating stronger ties and explicit roles in teams of rollers could allow further permutations of the reconfiguration that open up other parts of the task space.

Appendix A

Appendix

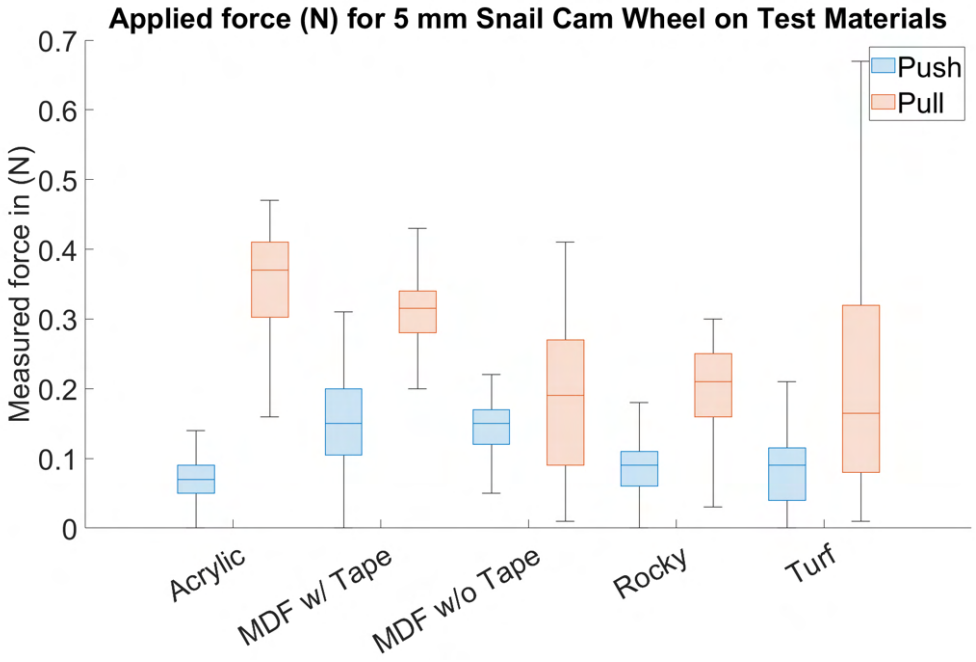

Figure A.1: 5mm eccentric snail cam pushing and pulling results. We see a cross material average pushing force of 0.11 N and a pulling force of 0.25 N.

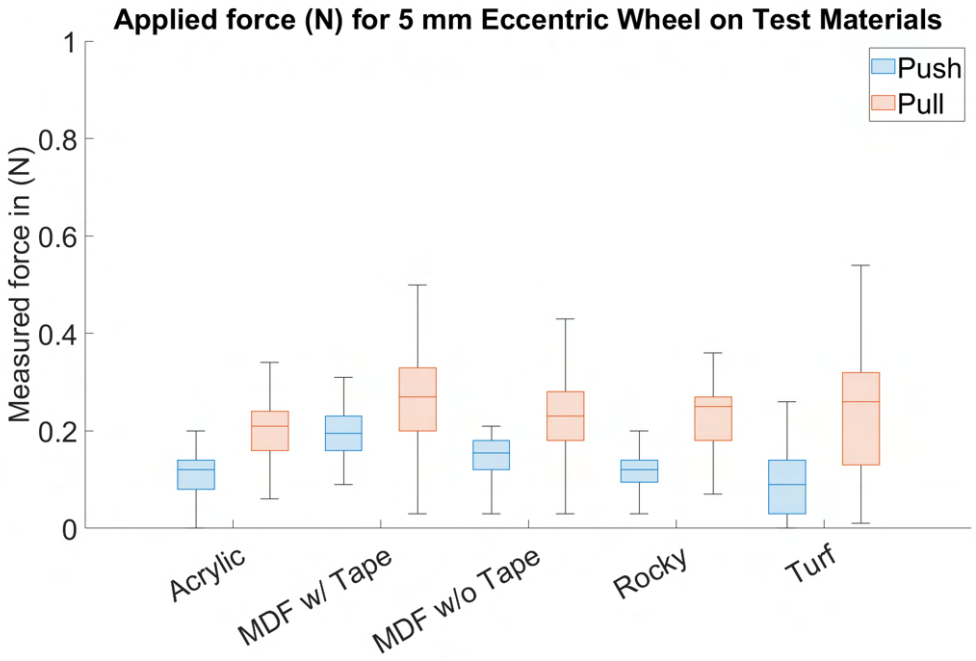

Figure A.2: 5mm Eccentric wheel pushing and pulling results. We see a cross material average pushing force of 0.13 N and a pulling force of 0.23 N.

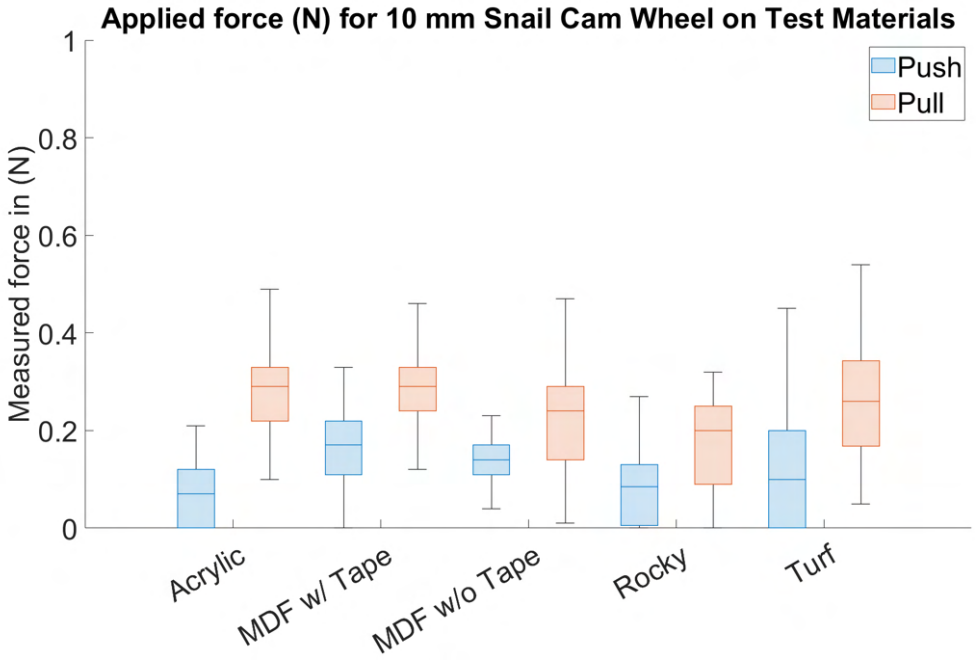

Figure A.3: 10 mm eccentric snail cam wheel pushing and pulling results. We see a cross material average pushing force of 0.11 N and a pulling force of 0.25 N.

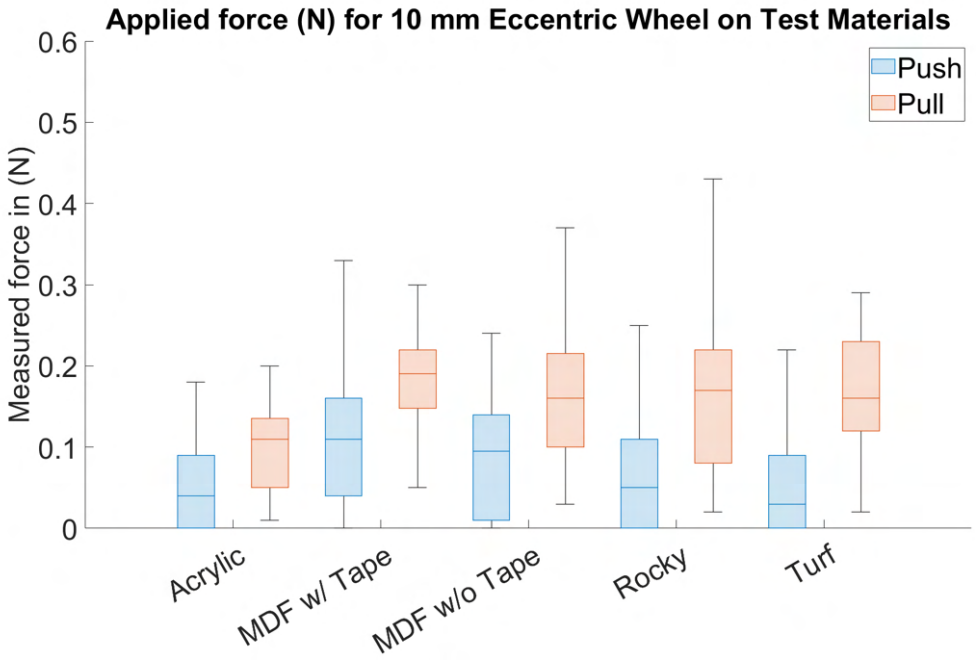

Figure A.4: 10 mm eccentric wheel pushing and pulling results. We see a cross material average pushing force of 0.07 N and a pulling force of 0.16 N.

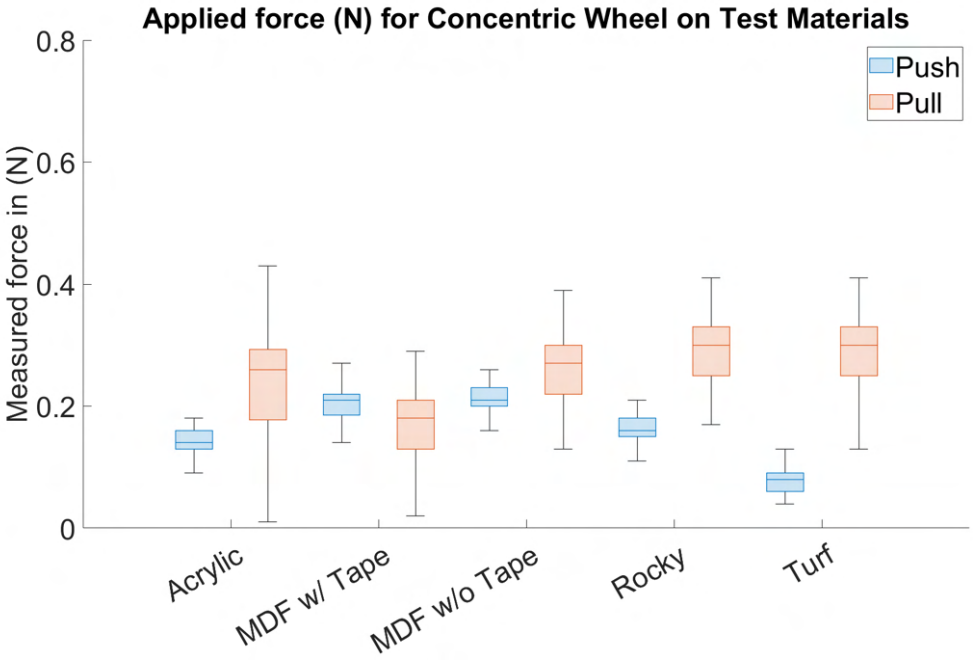

Figure A.5: Concentric wheel pushing and pulling results. We see a cross material average pushing force of 0.16 N and a pulling force of 0.25 N.

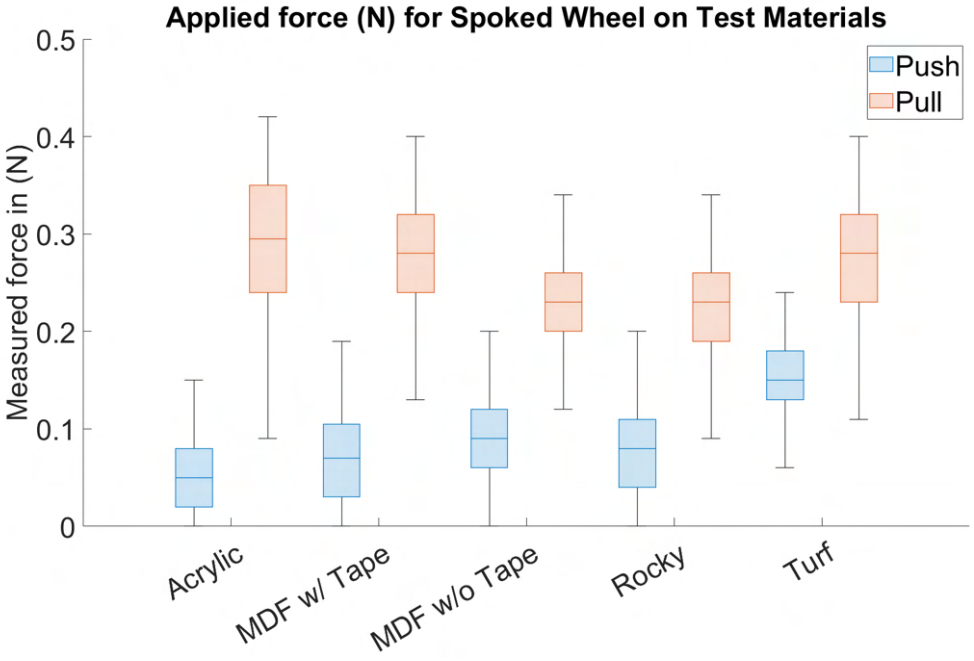

Figure A.6: Spoked wheel pushing and pulling results. We see a cross material average pushing force of 0.09 N and a pulling force of 0.25 N.

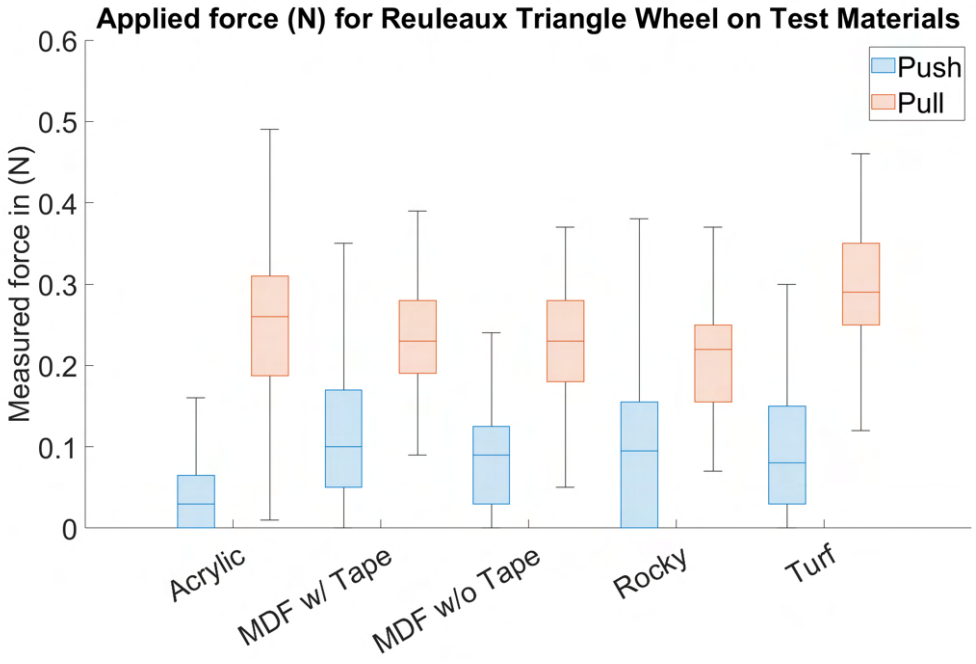

Figure A.7: Reuleaux wheel pushing and pulling results. We see a cross material average pushing force of 0.09 N and a pulling force of 0.24 N.

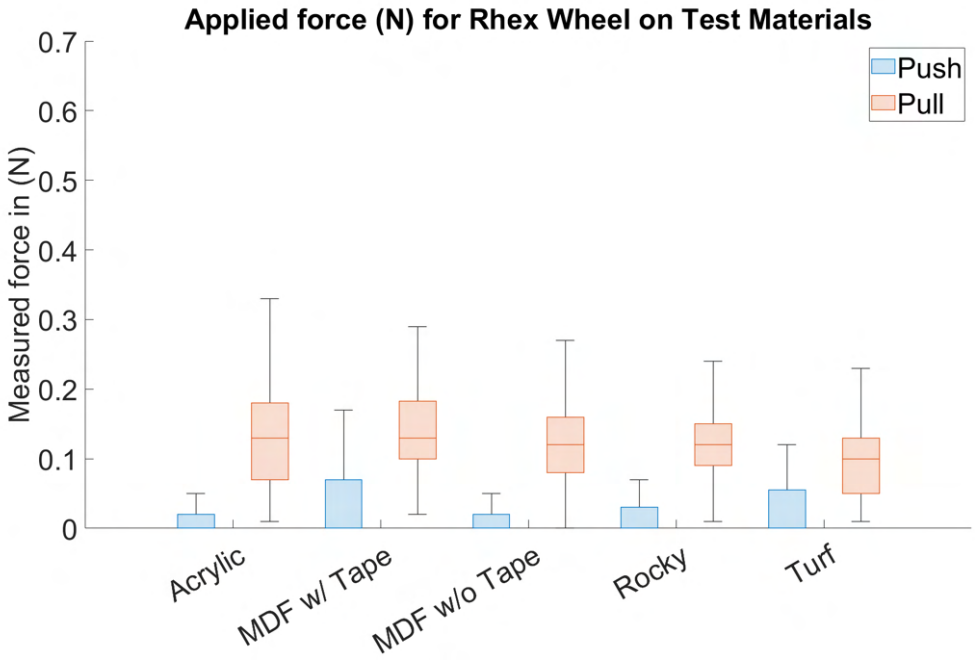

Figure A.8: Rhex wheel pushing and pulling results. We see a cross material average pushing force of 0.03 N and a pulling force of 0.13 N.

Figure A.9: Force testing materials. From left to right medium density fiberboard (MDF), our 3D printed “rocky” surface, LifeGrip tape on MDF, and turf.

Bibliography

[1] Precision compression spring: 0.3000˙00
Spring

[2] Laura H Blumenschein, Margaret M Coad, David A Haggerty, Allison M Okamura, and Elliot W Hawkes. Design, modeling, control, and application of everting vine robots. *Frontiers in Robotics and AI*, 7:548266, 2020. 2

[3] Jennifer Carlson and Robin R Murphy. How ugvs physically fail in the field. *IEEE Transactions on robotics*, 21(3):423–437, 2005. 3.0.2

[4] Margaret M Coad, Laura H Blumenschein, Sadie Cutler, Javier A Reyna Zepeda, Nicholas D Naclerio, Haitham El-Hussieny, Usman Mehmood, Jee-Hwan Ryu, Elliot W Hawkes, and Allison M Okamura. Vine robots. *IEEE Robotics & Automation Magazine*, 27(3):120–132, 2019. 1, 2, 4.4

[5] Jay Davey, Ngai Kwok, and Mark Yim. Emulating self-reconfigurable robots - design of the smores system. In *2012 IEEE/RSJ International Conference on Intelligent Robots and Systems*, pages 4464–4469, 2012. doi: 10.1109/IROS.2012.6385845. 4.1

[6] Pascal Auf der Maur, Betim Djambazi, Yves Haberthür, Patricia Hörmann, Alexander Kübler, Michael Lustenberger, Samuel Sigrist, Oda Vigen, Julian Förster, Florian Achermann, et al. Roboa: Construction and evaluation of a steerable vine robot for search and rescue applications. In *2021 IEEE 4th International Conference on Soft Robotics (RoboSoft)*, pages 15–20. IEEE, 2021. 2

[7] DIY. Diy magnetic connector - right angle, 2025. URL https://www.adafruit.com/product/5358. 4.5

[8] Marco Dorigo, Guy Theraulaz, and Vito Trianni. Reflections on the future of swarm robotics. *Science Robotics*, 5(49):eabe4385, 2020. 2

[9] Daniel S Drew. Multi-agent systems for search and rescue applications. *Current Robotics Reports*, 2:189–200, 2021. 2

[10] Dania Eridani, Adian Fatchur Rochim, and Faiz Noerdiyan Cesara. Compara-

tive performance study of esp-now, wi-fi, bluetooth protocols based on range, transmission speed, latency, energy usage and barrier resistance. In *2021 International Seminar on Application for Technology of Information and Communication (iSemantic)*, pages 322–328, 2021. doi: 10.1109/iSemantic52711.2021.9573246. 4.5

[11] Ronald S. Fearing. Challenges for efffective millirobots. In *2006 IEEE International Symposium on MicroNanoMechanical and Human Science*, pages 1–5, 2006. doi: 10.1109/MHS.2006.320303. 1, 5

[12] Elliot W Hawkes, Laura H Blumenschein, Joseph D Greer, and Allison M Okamura. A soft robot that navigates its environment through growth. *Science Robotics*, 2(8):eaan3028, 2017. 1, 2, 4.4

[13] Yong He, Wenping Wang, Qiang Wang, and Yujun Wang. Novel design of the wheel-footed obstacle-surmounting robot. In *Journal of Physics: Conference Series*, volume 1550, page 022019. IOP Publishing, 2020. 3.0.3

[14] Marco Hutter, Christian Gehring, Dominic Jud, Andreas Lauber, C. Dario Bellicoso, Vassilios Tsounis, Jemin Hwangbo, Karen Bodie, Peter Fankhauser, Michael Bloesch, Remo Diethelm, Samuel Bachmann, Amir Melzer, and Mark Hoepflinger. Anymal - a highly mobile and dynamic quadrupedal robot. In *2016 IEEE/RSJ International Conference on Intelligent Robots and Systems (IROS)*, pages 38–44, 2016. doi: 10.1109/IROS.2016.7758092. 2

[15] Adam Jacoff, Elena Messina, and John Evans. A standard test course for urban search and rescue robots. *NIST special publication SP*, pages 253–259, 2001. 2

[16] M.W. Jorgensen, E.H. Ostergaard, and H.H. Lund. Modular atron: modules for a self-reconfigurable robot. In *2004 IEEE/RSJ International Conference on Intelligent Robots and Systems (IROS) (IEEE Cat. No.04CH37566)*, volume 2, pages 2068–2073 vol.2, 2004. doi: 10.1109/IROS.2004.1389702. 4.1

[17] Brian T. Kirby, Burak Aksak, Jason D. Campbell, James F. Hoburg, Todd C. Mowry, Padmanabhan Pillai, and Seth Copen Goldstein. A modular robotic system using magnetic force effectors. In *2007 IEEE/RSJ International Conference on Intelligent Robots and Systems*, pages 2787–2793, 2007. doi: 10.1109/IROS.2007.4399444. 4.1

[18] Dae-Young Lee, Sareum Kim, Ji-Suk Kim, Jae-Jun Park, and Kyu-Jin Cho. Origami wheel transformer: A variable-diameter wheel drive robot using an origami structure. *Soft Robotics*, 4, 05 2017. doi: 10.1089/soro.2016.0038. 1

[19] Jae-Young Lee, Seongji Han, Munyu Kim, Yong-Sin Seo, Jongwoo Park, Dong Il Park, Chanhun Park, Hyunuk Seo, Joonho Lee, Hwi-Su Kim, Jeongae Bak, Hugo Rodrigue, Jin-Gyun Kim, Joono Cheong, and Sung-Hyuk Song. Variable-stiffness–morphing wheel inspired by the surface tension of a liquid droplet.

Science Robotics, 9(93):eadl2067, 2024. doi: 10.1126/scirobotics.adl2067. URL https://www.science.org/doi/abs/10.1126/scirobotics.adl2067. 1

[20] Jose León, Gustavo A Cardona, Andres Botello, and Juan M Calderón. Robot swarms theory applicable to seek and rescue operation. In *Intelligent Systems Design and Applications: 16th International Conference on Intelligent Systems Design and Applications (ISDA 2016) held in Porto, Portugal, December 16-18, 2016*, pages 1061–1070. Springer, 2017. 2

[21] Guanqi Liang, Haobo Luo, Ming Li, Huihuan Qian, and Tin Lun Lam. Freebot: A freeform modular self-reconfigurable robot with arbitrary connection point-design and implementation. In *IEEE/RSJ Int. Conf. Intell. Robots Syst., Las Vegas, USA*, 2020. 1, 4.1

[22] Nir Meiri and David Zarrouk. Flying star, a hybrid crawling and flying sprawl tuned robot. In *2019 International Conference on Robotics and Automation (ICRA)*, pages 5302–5308, 2019. doi: 10.1109/ICRA.2019.8794260. 1

[23] Robin R Murphy. *Disaster robotics*. MIT press, 2017. 2, 2, 3.0.2, 3.0.3

[24] L David Roper. Physics of automobile rollovers, 2001. 4.4

[25] Tomáš Rouček, Martin Pecka, Petr Čížek, Tomáš Petříček, Jan Bayer, Vojtěch Šalanský, Daniel Heřt, Matěj Petrlík, Tomáš Báča, Vojěch Spurný, François Pomerleau, Vladimír Kubelka, Jan Faigl, Karel Zimmermann, Martin Saska, Tomáš Svoboda, and Tomáš Krajník. Darpa subterranean challenge: Multi-robotic exploration of underground environments. In Jan Mazal, Adriano Fagiolini, and Petr Vasik, editors, *Modelling and Simulation for Autonomous Systems*, pages 274–290, Cham, 2020. Springer International Publishing. ISBN 978-3-030-43890-6. 1, 2, 2

[26] Uluc Saranli, Martin Buehler, and Daniel E Koditschek. Rhex: A simple and highly mobile hexapod robot. *The International Journal of Robotics Research*, 20(7):616–631, 2001. 3.0.3, 3.0.3

[27] Eric Sihite, Arash Kalantari, Reza Nemovi, Alireza Ramezani, and Morteza Gharib. Multi-modal mobility morphobot (m4) with appendage repurposing for locomotion plasticity enhancement. *Nature communications*, 14(1):3323, 2023. 1

[28] Shashwat Singh, Reed Truax, and Ryan St Pierre. Buffalo byte: A highly mobile and autonomous millirobot platform. *IEEE Robotics and Automation Letters*, 2024. 1

[29] Lauren M. Smith, Roger D. Quinn, Kyle A. Johnson, and William R. Tuck. The tri-wheel: A novel wheel-leg mobility concept. In *2015 IEEE/RSJ International Conference on Intelligent Robots and Systems (IROS)*, page 4146–4152. IEEE Press, 2015. doi: 10.1109/IROS.2015.7353963. URL https://doi.org/10.1109/IROS.2015.7353963. 3.0.3

[30] Ryan St. Pierre and Sarah Bergbreiter. Toward autonomy in sub-gram terrestrial robots. *Annual Review of Control, Robotics, and Autonomous Systems*, 2(1): 231–252, 2019. 1

[31] Milt Statheropoulos, Agapios Agapiou, George C Pallis, Katerina Mikedi, Sofia Karma, J Vamvakari, Miranda Dandoulaki, Fivos Andritsos, and CL Paul Thomas. Factors that affect rescue time in urban search and rescue (usar) operations. *Natural Hazards*, 75:57–69, 2015. 2

[32] Takara Tomy. SORA-Q. https://www.takaratomy.co.jp/english/products/sora-q/. Accessed: 2025-03-31. 3.0.3

[33] Marco Tranzatto, Takahiro Miki, Mihir Dharmadhikari, Lukas Bernreiter, Mihir Kulkarni, Frank Mascarich, Olov Andersson, Shehryar Khattak, Marco Hutter, Roland Siegwart, and Kostas Alexis. Cerberus in the darpa subterranean challenge. *Science Robotics*, 7(66):eabp9742, 2022. doi: 10.1126/scirobotics.abp9742. URL https://www.science.org/doi/abs/10.1126/scirobotics.abp9742. 1, 2

[34] Giorgio Valsecchi, Ruben Grandia, and Marco Hutter. Quadrupedal locomotion on uneven terrain with sensorized feet. *IEEE Robotics and Automation Letters*, 5(2):1548–1555, 2020. doi: 10.1109/LRA.2020.2969160. 2

[35] Hongxing Wei, Youdong Chen, Jindong Tan, and Tianmiao Wang. Sambot: A self-assembly modular robot system. *IEEE/ASME Transactions on Mechatronics*, 16(4):745–757, 2011. doi: 10.1109/TMECH.2010.2085009. 1, 4.1

[36] Sha Yi, Zeynep Temel, and Katia Sycara. Puzzlebots: Physical coupling of robot swarms. In *2021 IEEE International Conference on Robotics and Automation (ICRA)*, pages 8742–8748. IEEE, 2021. 1, 4.1